

ISSN 2658-3518

LIMNOLOGY & FRESHWATER BIOLOGY

2019, № 6

- > abiotic and biotic water components;
- > ecosystem-level studies;
- > systematics and aquatic ecology;
- > paleolimnology and environmental histories;
- > laboratory experiments and modeling

Dissolved methane in Lake Baikal: a modified technique for determining concentrations and vertical distribution in the water column

Mizandrontsev I.B.¹, Kozlov V.V.², Ivanov V.G.^{1*}, Kucher K.M.¹, Korneva E.S.¹, Granin N.G.¹

¹ Limnological Institute, Siberian Branch of the Russian Academy of Sciences, Ulan-Batorskaya Str., 3, Irkutsk, 664033, Russia

² Matrosov Institute for System Dynamics and Control Theory of Siberian Branch of Russian Academy of Sciences, Lermontov Str., 134, Irkutsk, 664033, Russia

ABSTRACT. We have developed a modified method of headspace analysis of water samples with the control of temperature and total pressure in the gaseous phase of a closed heterogeneous system followed by a gas chromatographic measurement of methane concentration with the methane content in the lake water of $< 500 \text{ nl CH}_4/\text{L}$. Here, we describe the background concentrations and vertical distribution of dissolved methane in the water column of Lake Baikal, which were obtained for several years.

Keywords: methane dissolved in water, vertical distribution, Lake Baikal, modified method of static headspace analysis

1. Introduction

The formation of the gas composition in surface natural waters occurs during the interaction of water bodies with the atmosphere, biochemical processes in the water column and bottom sediments as well as during metamorphization of rocks and degassing of mantle substances (Alekin, 1970). Under global warming and change in the concentrations of greenhouse gases in the atmosphere, the study of the composition and distribution of carbon dioxide and methane in the World Ocean and inland waters is of an undoubted scientific and practical interest.

East Siberian Branch of the Imperial Russian Geographical Society initiated the investigations of gases at Lake Baikal (Lomonosov and Chekanovsky, 1869; 1897). In the 1930s, significant attention was paid to oil and gas seepages at Lake Baikal (Ryabukhin, 1933; Vereshchagin, 1933). V.P. Isaev (2001) studied methane seepages in the Selenga shallow area. N.G. Granin and L.Z. Granina (2002) made a review of the available materials on the investigations of gas seepages in Baikal.

To determine the dissolved methane content in seawater and pore waters of sediments, oceanographers practise static headspace analysis (Bolshakov and Egorov, 1987; Vereshchagina et al., 2013) and vacuum extraction of gas (Obzhairov, 1993) followed by measurement of methane in gaseous phase with

gas chromatography-flame ionization detector (GC-FID). These techniques, which differ in the method for extracting the volatile component from the condensed phase, were used at Lake Baikal during the collaboration of Limnological Institute (LIN SB RAS) with oceanographers (Egorov et al., 2005; Granin et al., 2005; Schmid et al., 2007; Granin et al., 2013).

The first data on methane concentrations in the water and bottom sediments of Southern Baikal, estuarine areas of rivers and river-lake mixing zones were obtained in 1988 and 1994 (Fedorov et al., 1997)

The discoveries of methane hydrates (Golmshtok et al., 1997; Duchkov, 2003), mud volcanoes on the Baikal floor (Van Rensbergen et al., 2002) and hydrates in the surface sediments (Klerkx et al., 2003) initiated a systematic research of methane seepages from bottom sediments and methane distribution in the water column of the lake. In 2003, A.V. Egorov and coauthors (2005) studied methane in the samples from several stations of Southern Baikal.

In 2002-2004, researchers from the LIN SB RAS Laboratory of Hydrology and Hydrophysics together with researchers from Pacific Oceanological Institute Far Eastern Branch Russian Academy of Science (POI) investigated the methane content in the waters of all three basins of the lake. Background concentration of methane dissolved in water was determined by vacuum extraction of gas (Obzhairov, 1993) followed by the GC-FID measurement (Granin et al., 2005; Schmid

*Corresponding author.

E-mail address: vigo@lin.irk.ru (V.G. Ivanov)

et al., 2007; Granin et al., 2013). In 2013-2019, the investigations were continued.

The vacuum extraction of methane used in gas geochemistry studies to extract trace amount of dissolved gases from natural water and pore waters of bottom sediments, with all its advantages, requires special equipment and the extraction completeness control, which, according to (Bolshakov and Egorov, 1987), additionally complicates the operational processing of a large number of samples in expeditionary conditions. This led to the necessary use of a more efficient static headspace technique for gasometric studies (Bolshakov and Egorov, 1987; A technical guide ..., 2000; Kolb and Ettre, 2006; Boeva et al., 2012).

The standardized technique of (Boeva et al., 2012) yields good results at a concentration of methane dissolved in water of ≥ 500 nL CH₄ /L.

Our methodological work has revealed that at the background concentrations of 10-250 nL CH₄/L typical of the open Baikal waters, the conventional headspace analysis with helium (Vereshchagina et al., 2013) and air (Bolshakov and Egorov, 1987) yields underestimated results. Moreover, the calculated methane concentration decreases with an increase in the initial sample volume at a constant volume of the gas bubble. The stepwise calculation has indicated that the transition process from the initial state of a closed heterogeneous system (neutral individual dry gas – an aqueous solution with a mixture of atmospheric gases) to the dynamic equilibrium state is accompanied by the change in the total pressure in the gaseous phase. This inevitably affects the partial pressure of methane in both phases with the established equilibrium. Ignoring this fact leads to significant errors.

This study aims to develop modified static headspace analysis for detecting nanoconcentrations of dissolved methane with subsequent identification of the features in its content and vertical distribution in the water column of Lake Baikal.

2. Methods, equipment and calculations

The method is briefly described in (Mizandrontsev et al., 2020). Here, we describe the procedure of the proposed modification of headspace analysis, its theoretical justification, sample preparation, preparation of calibration gas mixtures and aqueous solutions with methane as well as methodological experiments.

The water from the lake was sampled using Niskin bathometers, and its temperature was simultaneously measured using a CTD probe (temperature can be also measured in a separate portion of water from the bathometer). A water sample was transferred through a hose attached to the bathometer with a twofold pouring to the 120 mL bottle. The bottle was closed with a rubber stopper (for penicillin bottles) with a syringe needle in the centre; then the needle was removed. The bottle was turned upside down to check for the absence of a gas bubble.

The stopper was fixed with the 20 mm aluminium cap having a round hole for syringes. This procedure is mandatory because in a closed system, the pressure changes during establishing the equilibrium state. The cap was crimped by collets (crimper hand sealing machine). Then, a needle of the empty syringe was inserted through the stopper for 5 mL (with a piston at zero value). Another needle was introduced, which was connected with a plastic bag filled with pure nitrogen (99.99% N₂ without CH₄) at atmospheric pressure. Using the syringe, 3 ml of water were slowly taken (to avoid the release of dissolved gases). They were synchronously replaced by 3 mL of pure nitrogen from the bag; then, the needles were removed from the stopper. Experiments with the 3 to 24 mL gas bubbles indicated that considering the measured pressure in the closed system, the results of the analysis are independent of the bubble volume and its radius.

K.M. Kucher, a researcher from the LIN SB RAS Laboratory of Hydrology and Hydrophysics, has developed a device that measures pressure in the gaseous phase of a closed system. The bottled samples prepared in this way were shaken on a shaker for one hour (four hours in methodological experiments with air without methane as the gaseous phase) until equilibrium in the heterogeneous system was established. Then, the final total pressure in the gaseous phase was measured. Using a syringe, 500 µg of the gaseous mixture were taken from the gaseous phase. In this mixture, molar (volume) fraction of methane was determined on an EKHO-PID GC-FID. The final temperature of the water in the bottle was measured immediately after sampling the gaseous phase for analysis.

In gas chromatographic measurements, the retention time of methane is 7.8-12 s. The isotherm is a fragment of a parabola with a slight deviation from linearity; the value of the signal/noise ratio varies from 6.5 at 11 nL CH₄/L to 200 at 465 nL CH₄/L; the relative error in determining methane concentration is $\pm 5\%$.

The chromatograph was calibrated according to the standards of LLC PGS-Service (Zarechny): Zero air (air + 4 ppm CH₄) and Nitrogen (N₂ + 8.6 ppm CH₄), as well as according to the standard Analysed Gases Scotty II mix 212 (100 ppm CH₄ in nitrogen) from Alltech Associates Inc. An additional test was carried out by determining the methane concentration at the equilibrium of distilled water with the atmosphere having constant atmospheric pressure and temperature, as well as by a saturated NaCl aqueous solution.

Methane concentration in water reduced to normal conditions, C_0 [nL CH₄/L H₂O], was calculated according to the formula based on the law of conservation of the methane mass in a closed system, Mendeleev-Clapeyron equation of state of a gas mixture, Bunsen solubility coefficients for methane, Henry's and Dalton's laws:

$$C_0 = \left(\frac{P_{en}}{101.325} - p_{en} \right) N_{en} \times 1000 \left(\alpha + \frac{273.15}{273.15 + t_{en}} \times \frac{V_g}{V_s - V_g} \right) - N_{in} \times 1000 \left(\frac{P_{in}}{101.325} - p_{in} \right) \times \frac{273.15}{273.15 + t_{in}} \times \frac{V_g}{V_s - V_g}, \quad (1)$$

where P is the measured total pressure in the system, [kPa]; p – the vapour pressure in the atmosphere units; α – the value of Bunsen absorption coefficient [L CH₄ /L H₂O] for methane at a temperature T [°K]; t – the temperature, [°C]; V_s – the initial volume of the water in a bottle before the formation of the gas bubble, [L]; V_g – the volume of the gaseous phase, [L]; 273.15 is the normal temperature T_0 , [°K]; and 101.325 is the normal pressure P_0 , [kPa]. Subscripts *in* and *en* correspond to initial and final state of the system; N_{en} is the volume (molar) fraction of methane measured on a chromatograph at the established phase equilibrium, [ppm_v]; N_{in} is the molar fraction of methane at the initial time, [ppm_v]. $N_{in} = 0$ when high purity nitrogen (helium, methane free air) is used to form the gas bubble in the bottle with the studied water. Because water expansion is small a narrow temperature range, the V_w and V_g are assumed to be constants.

The partial pressure of methane was calculated according to the following equation:

$$p_{gr} = N_{CH_4} \left(P_{mes} - \frac{h}{100} \cdot p_{vp} \right), \quad (2)$$

where N_{CH_4} is the molar (volume) fraction of methane in the gaseous phase determined using gas chromatography; P_{mes} – the total pressure in the gaseous phase measured by the device minus the vapour pressure p_{vp} ; and h – the humidity of the gaseous phase equal to 100% at the equilibrium.

The regression equations for the temperature dependence of the Bunsen coefficient for methane (Handbook of chemistry, 1964) and vapour pressure in the closed system, respectively, are as follows:

$$\alpha = 0.237329X^4 - 0.457531X^3 + 0.373582X^2 - 0.170859X + 0.055612, \quad (3)$$

$$p_{vp} = 0.597544X^4 + 0.140527X^3 + 0.157524X^2 + 0.043273X + 0.005999, \quad (4)$$

where $X = (T - T_0) / 100$.

According to Wiessenburg and Guinasso, 1979, α values in the range of 273.15 ÷ 303.15 °K:

$$\alpha = 0.548059X^4 - 0.681712X^3 + 0.427184X^2 - 0.176244X + 0.057378, \quad (3a)$$

differ from those of (3) by +3.2%.

In case of using pure nitrogen or methane free air to form the initial gaseous phase in a closed system, the initial value of the partial pressure of methane is zero, and in the application of standards, it is calculated considering the gaseous mixture ratings in the cylinder.

Preparation of gaseous standard solutions. An empty 34 ml calibrated bottle was closed with a rubber stopper, and a syringe needle was inserted there. Through another needle, the bottle was filled with pure nitrogen (methane free) from the cylinder. Then, both

needles were removed. A standard of 8.37 ppm CH₄, which is necessary to form the gaseous mixture with a given methane concentration, was inserted into the bottle with a syringe.

Several bottles were prepared containing gaseous solutions with methane concentrations ranging from 0.2 to 4.0 ppm:

amount of standard (mL)	31.1	18.9	14.5	19.7	7.4	4.6	2.2	1.7	1.3	0.8
resulting concentration (ppm)	4.0	3.0	2.5	2.0	1.5	1.0	0.5	0.4	0.3	0.2

Preparation of aqueous solutions with given methane concentrations. An aqueous solution with a methane concentration of 188.94 nL/L calculated according to (1) was prepared from the gaseous standard of 25 ppm. To do this, 1 mL standard was added with a syringe to the closed 120 mL bottle with distilled water, and 3 mL were replaced by high purity nitrogen. The initial temperature and total pressure in the closed system were measured. The bottle was shaken on a shaker for one hour to establish the equilibrium state in the gas-aqueous solution system. Before determining methane concentration in the gaseous phase, the pressure in the bottle was measured through chromatography, and then, the temperature in the bottle was measured.

The data on parallel measurements in 15 bottles enabled to calculate methane concentrations in the prepared aqueous solution. At a theoretical value of 188.94 nL/L, the measured concentration was 188.94 nL/L.

Similarly, two aqueous solutions with the calculated concentrations of 529.91 and 530.49 nL/L were prepared from the gaseous standard with a methane concentration of 70.81 ppm. In one of them, the average value from 15 measurements was 529.77 nL/L with a span of 3.65 nL/L, and in the other – 529.12 nL/L and 6.37 nL/L, respectively.

Choosing gas to form a gas bubble in a closed system. We carried out experiments to determine methane in water with the formation of a gas bubble from the air, methane free air, pure helium, and pure nitrogen. The static headspace measurements followed by gas chromatography of low methane concentrations in fresh water indicated that the use of pure nitrogen (99.99% N₂ without CH₄) or pure methane free air as a neutral gaseous phase yields stable results. At the same time, using nitrogen is more preferable, because the cost of the with pure nitrogen is much lower than the pure methane free air.

Pure helium as a neutral gas is inconvenient to form the initial gaseous phase due to its high volatility, which leads to the instability of the total pressure in the closed system. Atmospheric air as well as gaseous phase lead to significant error in measurements of methane concentrations at the equilibrium with atmosphere (at the Baikal level of ~100 nL CH₄ /L).

The device for measuring pressure in the gaseous phase of a closed heterogeneous gas-aqueous solution system of the gas mixture consists of an electronic absolute pressure sensor, a microcontroller, an indicator, and accumulator. All components of the device are arranged in a sealed housing that protects the electronics from moisture. Transparent walls of the housing allow reading pressure values on the indicator. Measurement unit is millibar (mbar). The precision of the pressure sensor is ± 2 mbar in the temperature range from 0 to 50°C. (In subsequent calculations, mbar are converted to atm).

The device is equipped with the Luer cone for the installation of standard medical needles that allow piercing the bottle's cap without loss of tightness. Internal volume of the pressure sensor and a needle is filled with liquid to minimize the error caused by the gas expansion into the measurement cavity. The integral battery allows the device to operate for two days; a standard mini USB connector is provided for charging.

The use of the device revealed the need for periodic replacement of needle due to clogging with pieces of rubber during piercing the caps. The clogging is easy to track when the pressure does not return to the atmospheric one between measurements.

Methodological experiments revealed that with control of the temperature and total pressure the change in the ratio of the volumes V_g and $V_w = V_s - V_g$ in the formula (1) does not affect the value of the determined methane concentration. The optimal V_w/V_g values are 10-40. The further decrease in the water volume to the volume of a gas bubble reduces the equilibrium volume concentration of methane in the gaseous phase to a level limited by ratings for chromatography.

Experimental assessment of the incomplete extraction of dissolved methane by vacuum method.

According to the extraction theory, the transition of a component from one phase of a heterogeneous system to another is never complete. Therefore, during vacuum extraction, standard experimentally established conditions should be met, which guarantee a sufficiently complete extraction of the investigated gas. Our modification of headspace outgassing does not require this. From the moment the dynamic equilibrium is established, the total pressure in the gaseous phase of a closed system becomes constant under invariable temperature.

A comparison of the results obtained using this modification of headspace analysis and single vacuum extraction has shown that the headspace analysis/vacuum extraction ratio is 1.39 ± 0.045 at a confidence level of 0.95, with a relative error of the average value of $\pm 3.2\%$. With two- and threefold extraction, the conversion factor approaches one. Previously (2002-2004), the correction for the incomplete extraction was assumed as 1.375 (Granin et al., 2005; Schmid et al., 2007).

Correlation of the results obtained by static headspace analysis with and without pressure control.

According to the methodological experiments with the gaseous phase of pure nitrogen, headspace outgassing without the temperature and pressure control in the closed system yields unstable results in determining the concentration of dissolved methane C^0 . The $C^0(P)/C^0$ ratio, where $C^0(P)$ is the concentration subject to pressure, varies from 1.1 to 1.6 (Fig. 1). Therefore, the average value of the conversion factor of C^0 into $C^0(P)$ is 1.35 with a maximum error of $\pm 20\%$, and the standard error of the average value should not exceed 10%.

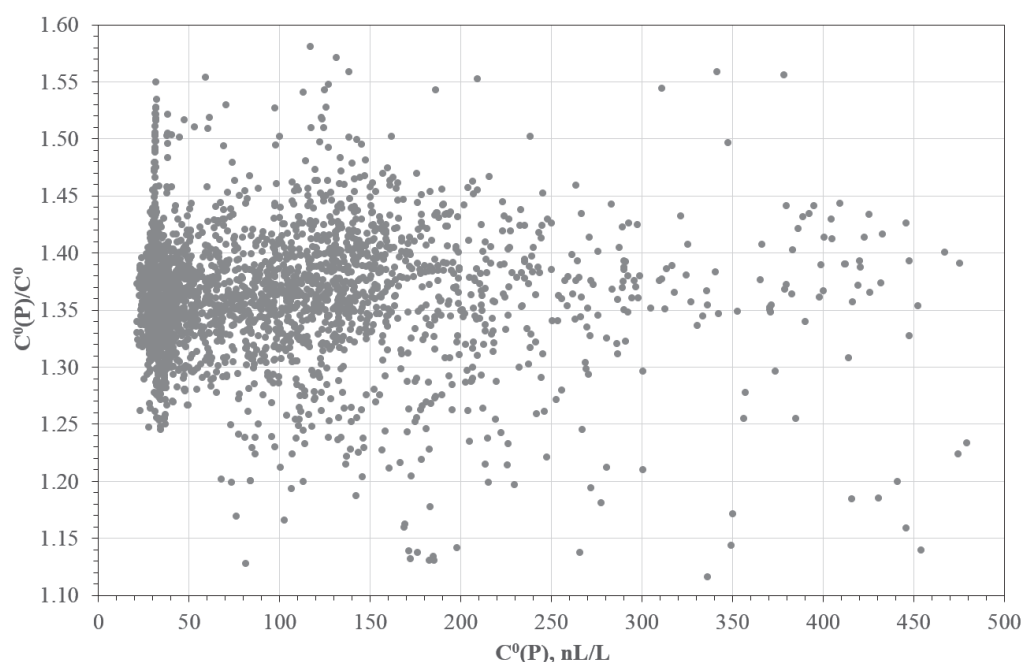


Fig. 1. Dependence of the ratio of the methane concentration determined with pressure $C^0(P)$ and without pressure control on the value C^0 .

Experimental data on air being the gaseous phase indicated that in this case, the $C^0(P)/C^0$ value varied from 0.5 to 3. In case of other gases used to form the gaseous phase, the conversion requires special experimental work to determine the $C^0(P)/C^0$ ratio.

Justification. Modified headspace analysis to determine low concentrations of methane dissolved in natural water (from tens to first hundreds of nL CH₄/L) is based on the law of the conservation of its mass in a closed system consisting of the gaseous phase and an aqueous solution with a gas mixture as well as on gas laws.

For example, there is a bottle of the V_s volume filled with an aqueous solution with a mixture of atmospheric gases. Dry individual gas free of the determined i -th gas replaces some part of this volume equal to V_g . Then, the formed heterogeneous system closes.

In the initially non-equilibrium closed system, the transition process begins to establish the thermodynamic equilibrium for all present gases, including water vapour. The gaseous phase takes the temperature of the aqueous phase. The amount of evaporating water comprises a small fraction of its volume. At a high heat capacity and low thermal expansion of water over a limited temperature range, the change in its volume V_w , as well as the volume V_g in the gaseous phase, can be neglected.

Mendeleev-Clapeyron equation describes the state of a mixture of ideal gases:

$$PV = NRT, \quad (5)$$

where P is the total pressure of the mixture; V is the volume of the mixture; $N = \sum_{i=1}^k n_i^{(g)}$ is the total number of gas moles in the gaseous phase; $n_i^{(g)}$ – the number of moles of the i -th gas in the mixture; R – the universal gas constant; and T – the absolute temperature. According to Dalton's law, the pressure of the gas mixture is equal to the sum of their partial pressures, $P = \sum_{i=1}^k p_i$. Thus, for the i -th gas, the equation of state is as follows:

$$p_i V = n_i^{(g)} RT, \quad (6)$$

In a closed system consisting of the aqueous solution with a mixture of gases and the gaseous phase, the total number of moles for the i -th gas is constant, $n_i = n_i^{(g)} + n_i^{(w)} = \text{const}$, but the current values, $n_i^{(g)}$ and $n_i^{(w)}$, change during the transition process. The calculations indicate that during the transition process, the total pressure P in the gaseous phase of the closed heterogeneous system increases sequentially due to the gas exchange between the phases and evaporation of water. The establishment of the constant value of the total pressure in the gaseous phase terminates

transition process. At the same time, the value of the partial pressure for each gas present in the system equalizes in both phases.

We solve the equation of state (6) relative to n_i and generate the expressions for the number of moles of the i -th gas in the aqueous solution and the gaseous phase. At the initial time, the total number of moles of the studied component in the heterogeneous system is

$$n_i = n_i^{(g)} + n_i^{(w)}, \text{ where } n_i^{(g)} = \frac{p_{inT_{in}}^{(g)} \cdot V_g}{R \cdot T_{in}}; n_i^{(w)} \text{ is the}$$

initial number of moles in the aqueous phase, whose volume is equal to the volume of the system V_s minus the volume of the introduced gas bubble V_g ; and $p_{inT_{in}}^{(g)}$ is the initial partial pressure of the i -th gas in the gaseous phase at the initial temperature T_{in} .

With the established equilibrium, the number of moles of a given gas in the gaseous phase and the aqueous solution is respectively as follows:

$$n_i^{(g)} = \frac{p_{iT_{en}}^{(g)} \cdot V_g}{R \cdot T_{en}} \text{ and } n_i^{(w)} = \frac{p_{iT_{en}}^{(g)} \cdot \alpha_{iT_{en}} \cdot V_w}{R \cdot T_0},$$

where according to (2) $p_{iT_{en}}^{(g)} = N_{CH_4} (P_{mes} - h/100 \cdot p_{wp})$

is its equilibrium partial pressure at the absolute temperature of measurement T_{en} ; V_g – the volume of the gaseous phase, V_w – the volume of the aqueous phase; $\alpha_{iT_{en}}$ – the Bunsen coefficient for the i -th gas; and $T_0 = 273.15$ °K – the normal temperature.

From the law of conservation of mass for the i -th gas, $n_i^{(g)} + n_i^{(w)} = n_{ie}^{(g)} + n_{ie}^{(w)}$, it follows that:

$$n_{in}^{(w)} = \frac{p_{iT_{en}}^{(g)} \cdot V_g}{R \cdot T_{en}} + \frac{p_{iT_{en}}^{(g)} \cdot \alpha_{iT_{en}} \cdot V_w}{R \cdot T_0} - \frac{p_{inT_{in}}^{(g)} \cdot V_g}{R \cdot T_{in}}, \quad (7)$$

At a zero initial concentration of the i -th gas in the gaseous phase (initially, this gas is absent in the gas bubble), the last summand in the equation vanishes. Otherwise (for example, during the calibration of chromatograph according to the standards), the value of this summand should be considered.

After reducing $n_i^{(w)}$ in moles to the dimension of the C_0 concentration in nmoles of CH₄ per one litre of water, we have $C_0 = n_i^{(w)} \frac{V_0}{V_w} 10^9$. The latter expression, considering (7) and the equation of state under normal conditions for one mole of gas, $V_0 p_0 = RT_0$, we reduce to the following expression:

$$C_0 = \frac{10^9 V_g}{V_w} \left[\left(\frac{p_{gT}}{p_0} \right) \cdot \alpha \frac{V_w}{V_g} + \left(\frac{p_{gT}}{p_0} \right) \cdot \frac{T_0}{T_{en}} - \left(\frac{p_{in gT}}{p_0} \right) \frac{T_0}{T_{in}} \right],$$

which considering (2), becomes (1) after the identical transformations.

3. Materials

In 2002-2004, during six cruises and winter expeditions on the ice, researchers from the LIN SB RAS Laboratory of Hydrology and Hydrophysics together with researchers from POI investigated 1280 water samples from all three Baikal basins for the background methane concentration (Granin et al., 2005; Schmid, et al., 2007; Granin et al., 2013). The bulk of the data was obtained from the water column of Southern Baikal. The background concentration of methane dissolved in water was determined by single vacuum extraction (Obzhirov, 1993) with the correction for the complete extraction of 1.375. Materials of the investigations were partially published in (Granin et al., 2005; Schmid et al., 2007; Granin et al., 2013).

In 2013-2019, the investigations were continued. Figure 2 shows the scheme of the stations where vertical water sampling was carried out. The methane concentration was determined by static headspace analysis with direct measurement of the total pressure in the closed gas-water system. The comparison of the methods has indicated that the ratio of the results of the headspace analysis/vacuum extraction having a confidence level of 0.95 is 1.39 ± 0.045 with a relative error of the average value of $\pm 3.2\%$. At the twofold extraction, the conversion factor of headspace analysis/twofold extraction is from 0.99 to 1.11 with the average value of ~ 1 .

4. Results and discussion

Procedure of static headspace analysis (Vitenberg and Ioffe, 1982; Vitenberg, 2003; Kolb and Ettre, 2006) used in oceanographic studies (Bolshakov and Egorov, 1987; Egorov, 2000; Vereshchagina et al., 2013) consists in single extraction of the investigated gas from the condensed phase into the gaseous phase followed by gas chromatographic determination of its concentration. In a closed system, which initially consists of an aqueous solution with atmospheric gases and neutral gaseous phase, phase equilibrium is established. Unlike the outgassing in a vacuum, this method does not require the mandatory assessment of the completeness in the extraction of the volatile component from the condensed phase into the gaseous phase.

The initial concentration of the investigated gas in the aqueous solution is calculated according to the basic formula for direct headspace analysis (Vitenberg and Ioffe, 1982):

$$C_w^0 = C_g \left(K + V_g / V_w \right), \quad (8)$$

where C_w^0 is the initial concentration of the determined gas in the condensed phase; C_g – its concentration in the gaseous phase; $K = C_w / C_g$ – the distribution coefficient of concentrations in phases; V_g and V_w – the volumes of the gaseous and aqueous phases, respectively. The formula (8) is valid at $K = \text{const}$, constant correlation of the volumes, compliance with isothermal conditions, and an invariable total pressure P in the system.

A theoretical analysis of the case when the total pressure P increases in the closed gas-liquid system under an isothermal regime with a decrease in the volume fraction of the gaseous phase was carried out in (Vitenberg and Marinichev, 1985). The change in P causes the associated changes in the equilibrium mass-volume concentration of the investigated volatile substance in the gaseous phase and the distribution coefficient K . Our direct measurements of the total pressure in the closed system have indicated that the change in the ratio of the volumes of the condensed and gaseous phases is accompanied by the change in the pressure at the established equilibrium (Fig. 3).

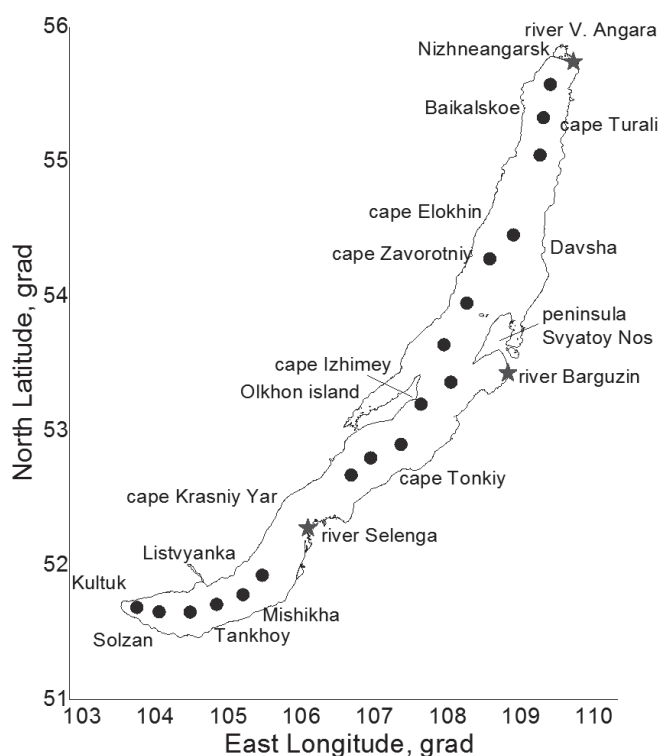


Fig. 2. The scheme of the water sampling stations for studying the background concentration and vertical distribution of methane in the water column of the lake (asterisks indicate large tributaries).

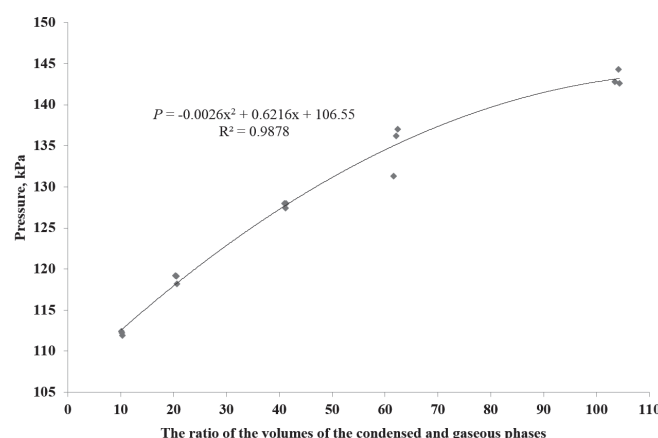


Fig.3. Dependence of the total pressure in the closed system of the gas and the aqueous solution with a gas mixture at the established phase equilibrium on the ratio of the volumes of the condensed and gaseous phases (according to Mizandrontsev et al., 2020).

Thus, the static headspace analysis with the gas chromatographic determination of low methane concentrations in natural water requires knowledge of the initial and final values the total pressure in a closed system as well as the initial and final temperature of the sample. These conditions are not provided in the methodologies by (Bolshakov and Egorov, 1987; Egorov, 2000; Vereshchagina et al., 2013), which leads to the errors in estimating the desired concentration of methane dissolved in water. Our methodological work revealed that measuring the concentration of methane dissolved in water through headspace analysis without control of the initial and final values of the pressure and temperature in the closed system yields significantly underestimated and unstable results in the range from 10 to 300 nL CH₄/L. Moreover, the law of conservation of mass is not met: at a constant volume of the gaseous phase, an increase in the volume of the water sample is accompanied by a decrease in the CH₄ concentration determined in this sample (Fig. 4).

The results obtained by headspace analysis using pure nitrogen or methane-free air to form the initial gas bubble with measurement of the initial and final temperature but without the control of the change in the total pressure in the gaseous phase of the closed system underestimated significantly the actual background concentration of dissolved oxygen in the water column of Lake Baikal (Fig. 4). The same measurements using gas bubble as the initial gaseous phase in the closed system without control of the total pressure showed a deviation towards a decrease in methane concentration by 30-70% at its content of 30-50 nL per one litre of water and by 20-40% at 100-150 nL CH₄/L).

Considering pressure and temperature during the establishment of the equilibrium in the closed system allow obtaining methane concentrations independent of the sample volume and the ratio of the gaseous and aqueous phases in the system. To demonstrate this, we analysed four series of water samples with different initial methane concentrations (Fig. 5).

Vertical methane distribution in open Baikal outside the zones of influence of tributaries, gas seeps and mud volcanoes shows the maximum value in the surface water (Fig. 6b, Fig. 6f) or the maximum concentrations in the subsurface layer of the water column with a subsequent decrease in the concentrations to the bottom in the main deep zone of the lake (Fig. 6a, Fig. 6b, Fig. 6c, Fig. 6e).

This distribution is similar to the type I methane distribution in oceans, which is observed at a low methane concentration (approximately 10⁻⁵ mL/L or less) that decreases from the near-surface layer to the bottom. Such distribution is the most widespread in the vast internal area of the ocean and is often found at its margins and in separate water areas of inland seas (Lamontagne et al., 1971; 1973; Geodekryan et al., 1979; Obzhairov et al., 2002).

In the main deep part of the water column of open Baikal, the concentration of dissolved methane are below equilibrium values with the atmosphere (~ 100 nL/L), which is due to the activity of aerobic methanotrophs (Hanson and Hanson, 1996; Galchenko,

2001). The *in situ* rate of methane oxidation in the lake was estimated in (Schmid et al., 2007; Granin et al., 2013).

In the near-bottom area, there is often a relatively slight increase in methane concentration under the influence of its flux from the bottom sediments (Fig. 6c, Fig. 6f). In some cases, this increase can be significant (Fig. 6d).

In the active layer of the lake (0-300 m), especially in its upper part, the concentrations of dissolved methane can significantly exceed their equilibrium value with the atmosphere. This is due to the methane paradox, i.e. methane generation in oxygen-saturated waters (Lamontagne et al., 1973; Oremland, 1979; Lilley et al., 1982; Schmidt and Conrad, 1993; Lein and Ivanov, 2005; Tang et al., 2014). In deep water of Lake Baikal, the formation of the near-surface methane maximum can be also associated with the decomposition of methane hydrates floating from the bottom (Granin et al., 2012). The causes and manifestations of methane paradox in Baikal will be discussed in the future article.

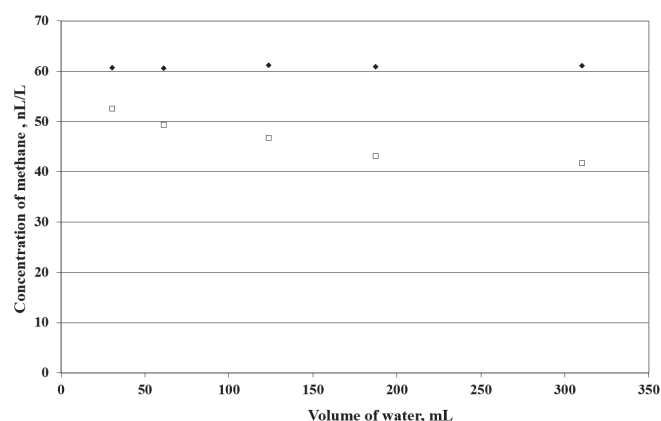


Fig. 4. Measured concentrations of dissolved methane with the control of the initial and final values of temperature and pressure in the closed system (black diamonds) and without pressure (squares). The volume of the gaseous phase (pure nitrogen) is 3 mL; the volume of water is variable (according to Mizandrontsev et al., 2020).

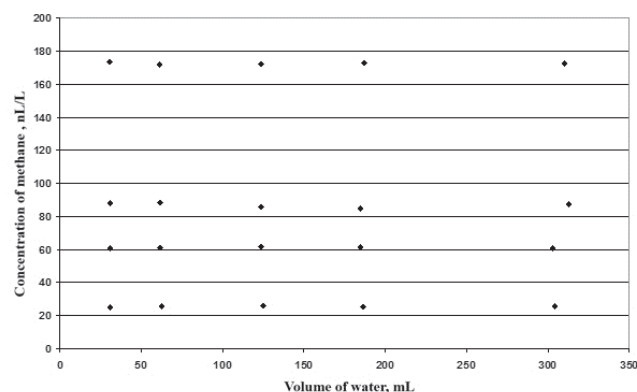


Fig. 5. Measured methane concentrations in different volumes of water considering the initial and final values of pressure and temperature in the closed system (initial gaseous phase is 3 mL of pure nitrogen).

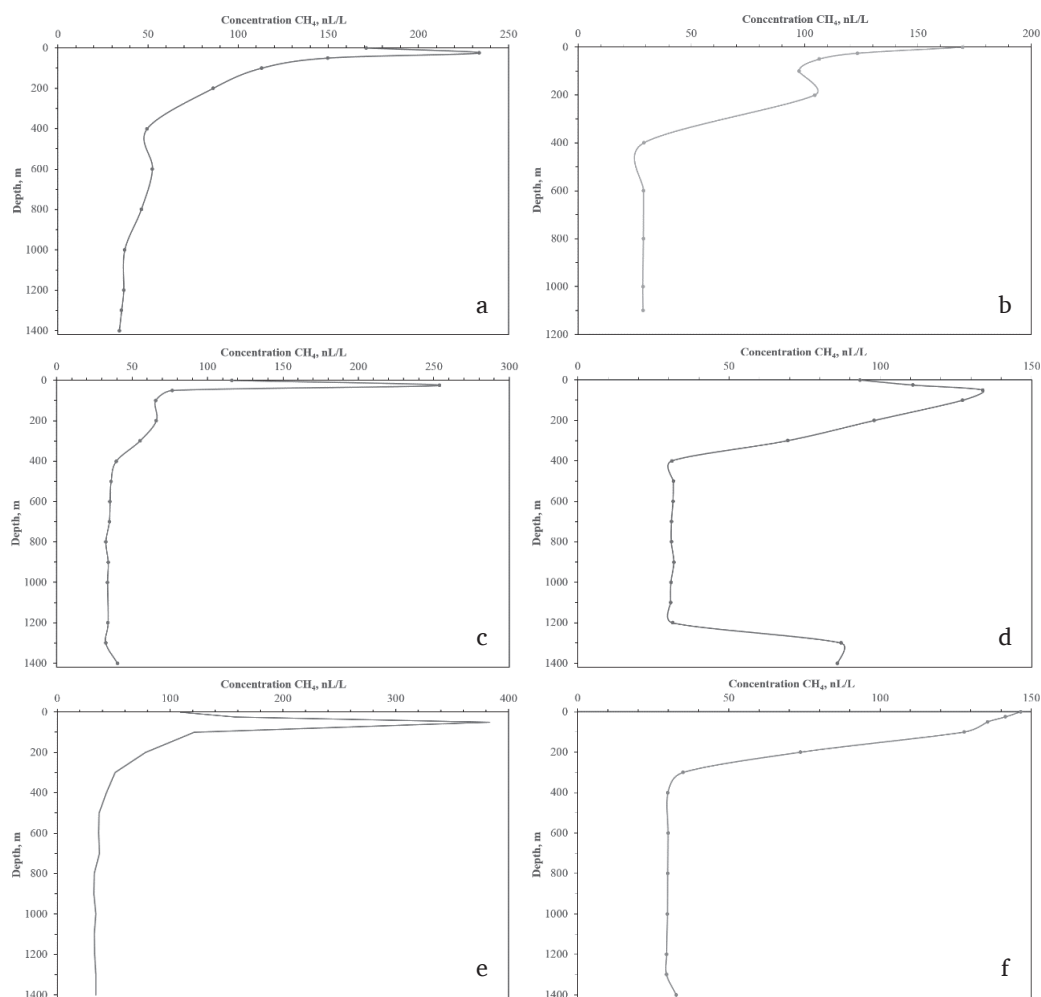


Fig.6. Examples of the vertical distribution of dissolved methane in the water column of different stations in Lake Baikal.

Increase in the concentrations of dissolved methane in the water column of the lake was observed in 2017-2019 in comparison with 2003 owing to its intensified discharge from the bottom sediments (Fig. 7). Methane concentration increased both in the deep zone of open Baikal (2-3 times higher on average) and its active layer (1.2-1.7 times higher).

The possible modern increase in methane concentration was discussed in (Granin et al., 2010; 2013). This phenomenon is likely due to the transition process initiated by the change in the water level of Lake Baikal after the launch of the Irkutsk Hydroelectric Power Station. As the water level rose, the boundary of the thermodynamic stability zone of methane hydrates in the stratum of the lake's bottom sediments shifted downwards. This led to the lowering the gas hydrates stability boundary. Due to this formation of gas hydrates have taken place at the lower boundary and the intensity of gas seepages decreased. At the end of the transition process, which lasted for a few tens of years pressure at the lower boundary of gas hydrate occurrence began to increase. It was accompanied by an increase in the intensity of gas seepages from the sediments and methane concentration in the water column.

Dissolved oxygen is transported into the water column of Lake Baikal through the weakened sediment areas associated with numerous faults during the

discharge of the products from the decomposition of gas hydrates (Levi et al., 1999). In this case, the upward flow of water and methane forms a secondary accumulation of methane in the near-surface zone of bottom sediments (Granin et al., 2012).

The activation of the gas bubbles also contributes to an increase in methane concentration. The transition process should terminate when a new equilibrium is established in the gas-water-gas hydrates system at the modern water level of Lake Baikal. Perhaps, the same transition process and its consequences can be observed in the Caspian Sea as a result of an increase in its water level.

5. Conclusion

We have developed the modified headspace analysis with the pressure and temperature control in the closed system of water and aqueous solution with atmospheric gases, which enables to obtain stable methane concentrations in natural water, with methane content ranging from 10 to 500 nL/L. The results of the analysis are independent of the ratio of the volumes of aqueous and gaseous phases. This modification of headspace analysis can be used to determine low concentrations of volatile components in an aqueous solution (trace gases and pollution components).

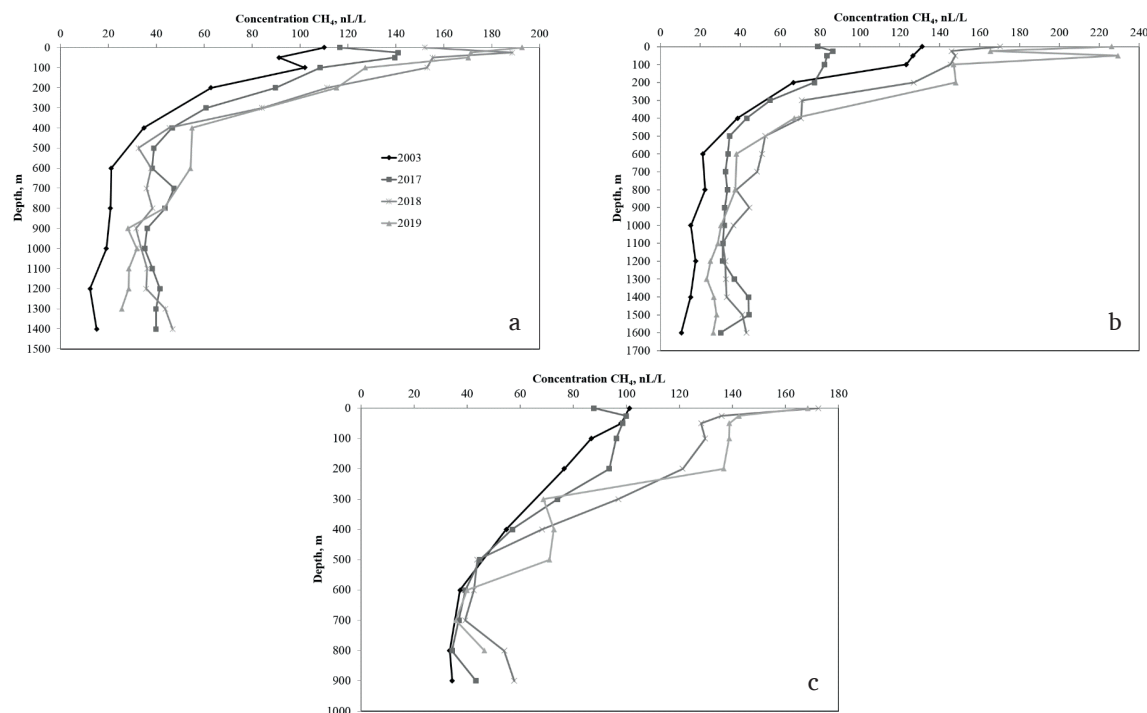


Fig.7. Increase of methane concentrations in the water column of open Baikal 2003-2019 (average for a – south, b – central, c- north, years on Fig. 7a).

Vertical distribution of dissolved methane in the water column of the lake is similar to that in oceans: methane concentration decreases from the top of the active layer to the lake floor. At depths from the surface layer to 150-200 m, there are the maximum methane concentrations. Sometimes, the maximum degenerates into its greatest value in the surface water.

Over the past decade, there was an increase in methane concentrations in the water column of open Baikal. This phenomenon is a consequence of the final stage of the transition process that was initiated by the rise in the water level of Baikal during the construction of the Irkutsk Hydroelectric Power Station.

Acknowledgements

The study was supported by project No. 0345-2019-0008.

References

- A technical guide for static headspace analysis using GC. 2000. Restek Corporation (www.restek.com)
- Alekin O.A. 1970. *Osnovy gidrokhimii*. Leningrad: Gidrometeoizdat. (in Russian)
- Boeva L.B., Tambieva N.S., Mikhailenko O.A. 2012. RD 52.24.512-2012. Volumetric concentration of methane in waters. Measurement technique by the gas chromatographic method using headspace analysis (Electronic text of the document). Ministry of Natural Resources and Ecology of the Russian Federation; Rosgidromet. Rostov-on-Don: FGU GHI. (in Russian)
- Bolshakov A.M., Egorov A.V. 1987. The use of phase equilibrium degassing techniques in gasometric studies. *Okeanologiya* [Oceanology] 27: 861-862. (in Russian)
- Duchkov A.D. 2003. Methane gas hydrates in sediments of Lake Baikal. *Rossiiskiy Khimicheskyy Zhurnal* [Russian Chemical Journal] 47: 91-100. (in Russian)
- Egorov A.V. 2000. Biogeochemistry of methane in the sediments of the Baltic and Black Seas: kinetic models of diagenesis. *Okeanologiya* [Oceanology] 40: 690-696. (in Russian)
- Egorov A.V., Zemskaya T.I., Grachev M.A. 2005. The main patterns of methane distribution in water and sediments of Lake Baikal. In: 4th Vereshchagin Baikal Conference, pp. 76-77.
- Fedorov Yu.A., Nikanorov A.M., Tambieva N.S. 1997. The first data on the distribution of biogenic methane content in water and bottom sediments of Lake Baikal. *Doklady Akademii Nauk* [Reports of the Academy of Sciences] 353: 394-397. (in Russian)
- Galchenko V.F. 2001. *Metanotrofnyye bakterii*. Moscow: GEOS. (in Russian)
- Geodekyan A.A., Trotsyuk V.Ya., Avilov V.I. et al. 1979. Hydrocarbon gases. In: Bordovsky O.K., Ivanenkov V.N. (Eds.), *Okeanologiya. Khimiya okeana. T. 1. Khimiya vody okeana*. Moscow, pp. 164-175. (in Russian)
- Golmshtok A.Ya., Duchkov A.D., Hutchinson D.R. et al. 1997. Estimates of the heat flux in Lake Baikal according to seismic data on the lower boundary of the gas hydrate layer. *Russian Geology and Geophysics* 10: 1677-1691. (in Russian)
- Granin N.G., Granina L.Z. 2002. Gas hydrates and escapes of gases in Lake Baikal. *Geologiya i Geofizika* [Russian Geology and Geophysics] 43: 629-637. (in Russian)
- Granin N.G., Mizandrontsev I.B., Obzhairov A.I. et al. 2005. Gas exchange of Baikal by methane with the atmosphere. In: 4th Vereshchagin Baikal Conference, pp. 56-57.
- Granin N.G., Suetnova E.I., Granina L.Z. 2010. Decomposition of gas hydrates in bottom sediments of Lake Baikal: possible causes and consequences. In: Joint International Conference "Minerals of ocean – 5 and Deep-sea minerals and mining – 2", pp. 110-116.
- Granin N.G., Muyakshin S.I., Makarov M.M. et al. 2012. Estimation of methane fluxes from bottom sediments of Lake Baikal. *Geo-Marine Letters* 32: 427-436. DOI: 10.1007/s00367-012-0299-6

- Granin N.G., Mizandrontsev I.B., Obzhairov A.I. et al. 2013. Oxidation of methane in the water column of Lake Baikal. *Doklady Earth Sciences* 451: 784-786. DOI: 10.1134/S1028334X13070258
- Handbook of chemistry. Vol. 3. 1964. Moscow-Leningrad: Khimiya. (in Russian)
- Hanson R.S., Hanson T.E. 1996. Methanotrophic bacteria. *Microbiology Reviews* 60: 439-471.
- Isaev V.P. 2001. Gas paleovolcanism at Lake Baikal. *Geologiya Nefti i Gaza [Geology of Oil and Gas]* 5: 45-50. (in Russian)
- Klerkx Ya., Zemskaya T.I., Matveeva T.V. et al. 2003. Methane hydrates in deep bottom sediments of Lake Baikal. *Doklady Earth Sciences* 393: 1342-1346.
- Kolb B., Ettre L.S. 2006. Static headspace-gas chromatography, theory and practice. NY: John Wiley & Sons.
- Lamontagne R.A., Swinnerton J.W., Linnenbom V.J. 1971. Nonequilibrium of CO and CH₄ at the air-water interface. *Journal of Geophysical Research* 78: 5117-5131.
- Lamontagne R.A., Swinnerton J.W., Linnenbom V.J. et al. 1973. Methane concentration in various marine environments. *Journal of Geophysical Research* 78.: 5317-5324.
- Lein A.Yu., Ivanov M.V. 2005. The largest methane water body on the Earth. *Priroda [Nature]* 2: 19-25. (in Russian)
- Levi K.G., Miroshnichenko A.I., Ruzhich V.V. et al. 1999. Modern faulting and seismicity in the Baikal Rift. *Fizicheskaya Mekhanika [Physical Mechanics]* 2: 171-180. (in Russian)
- Lilley M.D., Baross J.A., Gordon L.I. 1982. Dissolved hydrogen and methane in Saanich Inlet, British Columbia. *Deep-Sea Research* 29: 1471-1484.
- Lomonosov A.M., Chekanovsky A.L. 1869. The gases emitted from the bottom of Lake Baikal. *Izvestiya Rossiiskogo Imperatorskogo Geograficheskogo Obshchestva [Proceedings of the Russian Imperial Geographical Society]* 5, Baikal issue I: 67-76. (in Russian)
- Lomonosov A.M., Chekanovsky A.L. 1897. The gases emitted from the bottom of Baikal. *Izvestiya Rossiiskogo Imperatorskogo Geograficheskogo Obshchestva [Proceedings of the Russian Imperial Geographical Society]* 1, Baikal issue I: 137-145. (in Russian)
- Mizandrontsev I.B., Kozlov V.V., Ivanov V.G. et al. 2020. The vertical distribution of methane in the water column of Lake Baikal. *Water Resources* 47: 122-129. DOI: 10.1134/S0097807820010108
- Obzhairov A.I. 1993. *Gazogeokhimicheskiye polya pridonnogo sloya morey i okeanov*. Moscow: Nauka. (in Russian)
- Obzhairov A.I., Vereshchagina O.F., Suess E. et al. 2002. Methane distribution in the water columns of the eastern shelf and the Sakhalin slope in the Sea of Okhotsk in different seasons of 1998-2000. In: Obzhairov A.I., Salyuk A.N., Vereshchagina O.F. (Eds.), *Methane monitoring in the Sea of Okhotsk*. Vladivostok, pp. 8-37. (in Russian)
- Oremland R.S. 1979. Methanogenic activity in plankton samples and fish intestines: A mechanism for in situ methanogenesis in oceanic surface waters. *Limnology and Oceanography* 24: 1136-1141.
- Ryabukhin G.E. 1933. A note on the combustible gases of Lake Baikal. *Na Geologicheskoy Fronte Vostochnoy Sibiri [On the Geological Front of Eastern Siberia]* 1: 106-112. (in Russian)
- Schmid M., De Batist M., Granin N.G. et al. 2007. Sources and sinks of methane in Lake Baikal: A synthesis of measurements and modeling. *Limnology and Oceanography* 52: 1824-1837. DOI: 10.4319/lo.2007.52.5.1824
- Schmidt U., Conrad R. 1993. Hydrogen, carbon monoxide, and methane dynamics in Lake Constance. *Limnology and Oceanography* 38: 1214-1226. DOI: 10.4319/lo.1993.38.6.1214
- Tang K.W., McGinnis D.F., Frindte K. et al. 2014. Paradox reconsidered: Methane oversaturation in well-oxygenated lake waters. *Limnology and Oceanography* 59: 275-284. DOI: 10.4319/lo.2014.59.1.0275
- Van Rensbergen P., De Batist M., Klerkx J. et al. 2002. Sublacustrine mud volcanoes and methane seeps caused by dissociations of gas hydrates in Lake Baikal. *Geology* 30: 631-634. DOI: 10.1130/0091-7613(2002)030<0631:SMVA MS>2.0.CO;2
- Vereshchagin G.Yu. 1933. Gases from the bottom of Lake Baikal and on its coast. In: Lukashuk A.I., Vereshchagin G.Yu. (Eds.), *Prirodnyye gazy SSSR. T. 27. Pribaikalye*. (in Russian)
- Vereshchagina O.F., Korovitskaya E.V., Mishukova G.I. 2013. Methane in water columns and sediments of North Western Sea of Japan. *Deep-Sea Research Part II: Topical Studies in Oceanography* 86-87: 25-33. DOI: 10.1016/j.dsr2.2012.08.017
- Vitenberg A.G. 2003. Static headspace gas chromatography. *Physicochemical fundamentals and applications*. *Rossiiskiy Khimichesky Zhurnal [Russian Chemical Journal]* 47: 7-22. (in Russian)
- Vitenberg A.G., Ioffe B.V. 1982. *Gazovaya ekstraktsiya v khromatograficheskom analize*. Leningrad: Khimiya. (in Russian)
- Vitenberg A.G., Marinichev A.N. 1985. The effect of changes in total pressure on the accuracy of headspace gas chromatography. *Doklady Akademii Nauk [Reports of the Academy of Sciences]* 282: 353-358. (in Russian)
- Wiessenburg D.A., Guinasso N.L. 1979. Equilibrium solubility of methane, carbon dioxide, and hydrogen in water and sea water. *Journal of Chemical & Engineering Data* 24: 356-360.

Telomere length decreases during early life stages in peled

Koroleva A.G.*, Sapozhnikova Yu.P., Tyagun M.L., Gasarov P.V., Glyzina O.Yu., Sukhanova L.V., Kirilchik S.V.

Limnological Institute, Siberian Branch of the Russian Academy of Sciences, Ulan-Batorskaya Str., 3, Irkutsk, 664033, Russia

ABSTRACT. The different type of the age-related dynamics of telomeric DNA in different species indicates the complex mechanisms for regulating telomere length. In fish, telomere length can decrease, be maintained or increase during ontogeny. The cause of this is still unclear, but we assume that the regulation of telomeric DNA length may depend on the activity of protective systems and distribution of energy resources between tissues. We studied age-related dynamics of telomeric DNA in muscles and fins of peled, *Coregonus peled*, a valuable commercial fish that is widespread in the Russian North and used for successful acclimatization. Using quantitative PCR, we revealed a shortening of telomeric DNA in both tissues during the first two years of life of peled. Perhaps, a pattern of telomeric DNA dynamics is associated with the species-specific features of growth and development since some other salmonids maintain telomere length in the first years of life.

Keywords: telomere length, telomere dynamics, age, *Coregonus peled*

1. Introduction

In the 1960s, L. Hayflick and co-authors published the data showing that human diploid cells divide approximately 50 times (Hayflick and Moorhead, 1961; Hayflick, 1965). This doubling limit of somatic cells is now called the Hayflick limit and associated with the end-replication problem (Olovnikov, 1971; 1973). At the ends of chromosomes, DNA has a special structure and together with proteins forms telomeres (de Lange, 2005). Telomeres protect the rest of DNA from degradation and prevent fusion of chromosomes with each other (Deng and Chang, 2007). Due to the end-replication problem, each cell division leads to a decrease in telomeres. This enables considering telomeres as a mitotic clock, on which the proliferative potential of cells depends (Harley et al., 1990; Allsopp et al., 1992). The obtained data allowed telomeres to be attributed to one of the nine key biomarkers of ageing (López-Otín et al., 2013). At the same time, there are some examples in various taxonomic groups when the age-related dynamics of telomeric DNA (tDNA) has a different type: in mollusks (Gruber et al., 2014; Maximova et al., 2017), fish (Gao and Munch, 2015), reptiles (Paitz et al., 2004), birds (Caprioli et al., 2013), etc. Normally, tDNA dynamics is associated with telomerase activity, an enzyme that maintains the telomere length (Greider and Blackburn,

1989). However, cases when telomeres can decrease in the presence of active telomerase indicate the more complex mechanism for regulating the length of tDNA (Hatakeyama et al., 2008; Hartmann et al., 2009). External and internal factors, such as UV and radiation, intense sound, temperature, or oxidative stress (Oikawa et al., 2001; Doroshuk et al., 2013; Injaian et al., 2019; Singh et al., 2019), can also influence the length of tDNA, which partly explains the loss of telomeric repeats in non-dividing cells.

tDNA of vertebrates consists of short TTAGGG repeats and has different lengths, depending on species (Meyne et al., 1989; Gomes et al., 2011; de Abechuco et al., 2016). Fish were the first vertebrates that showed a decrease in tDNA in the presence of active telomerase (Hatakeyama et al., 2008; Hartmann et al., 2009). Telomerase can perform functions that are not related to maintaining telomeres and be involved in the regulation of the cell cycle, proliferation, regeneration, apoptosis, and some other processes (Romaniuk et al., 2019). Therefore, the presence of active telomerase does not guarantee the maintenance of telomeres and, hence, the absence of the Hayflick limit. A decrease in telomeres is rather associated with tissue type and metabolic characteristics than proliferative potential, as shown for *Danio rerio* Hamilton 1822 (Carneiro et al., 2016). Fish belong to animals with a very high phenotypic plasticity, which is evolutionarily associated

*Corresponding author.

E-mail address: ankor-2015@yandex.ru (A.G. Koroleva)

with their strong dependence on environmental conditions (Woodhead, 1998). On the one hand, the constant growth typical of fish along with a need to respond to stresses loads the replicative and preparative systems of cells in some tissues and can decrease tDNA (Hatakeyama et al., 2008; Carneiro et al., 2016). On the other hand, there are some examples when tDNA does not decrease in fish (Horn et al., 2008; Izzo et al., 2014; Gao and Munch, 2015). This can be due to the different activities of telomerase, which in one case maintains telomeres, and in other cases, it does not. Nevertheless, we should not exclude the more complex mechanism for regulating tDNA dynamics involving many factors.

Coregonus peled Gmelin 1789 is species of whitefish that is widespread in the Russian North. Peled tolerates significant fluctuations in temperature and water composition. It also has a wide nutrition spectrum, and with feed abundance, it can quickly gain weight. Owing to these abilities, this fish acclimatizes well and currently inhabits various water bodies of Russia and other countries (Mukhachev, 2003). Members of the order Salmoniformes, *Oncorhynchus kisutch* Walbaum 1792 and *Salmo trutta* Linnaeus 1758, maintain the telomere length during first years of life (Naslund et al., 2015; Pauliny et al., 2015). This study aimed to assess the age-related dynamics of tDNA in *C. peled*, other valuable salmonid species.

2. Materials and methods

The study material was brought from the Belsk fish hatchery (Irkutsk Region, Usolsky District, Baikalskaya Ryba LLC). Until the analysis, the material was kept in the unique facility “Experimental freshwater aquarium complex of Baikal hydrobionts” at Limnological Institute SB RAS. Eggs and larvae of peled were kept at a temperature of 4-5°C; fish – in a pool with a water temperature of ~15°C. Individuals in three stages of ontogeny were selected: eggs (five-six months, n = 29), larvae (one-two days after hatching, n = 26) and two-year individuals (n = 22). Among them, there were females and males in the maturity stages I-II. To analyze the length of telomeres, we used white muscles (for individuals in all three stages) and fins (for larvae and two-year adults).

Genomic DNA was extracted using the phenol/chloroform method (Sambrook et al., 1989) because it allows obtaining DNA samples of high quality (Voropaeva et al., 2015). Relative telomere length (telomere DNA concentration/ DNA concentration of single copy-gene, T/S) was measured by qPCR as described in Cawthon, 2002. The qPCR was carried out using the Rotor-Gene Q 6000 (QIAGEN, Germany). The gene of GAPDH served as a reference gene. Primer pair was designed using the gene sequence of Atlantic salmon (BT045621). Primer sequences were GCACTCACACCCTCCATAAC (forward) and ACAGCCTACGACAGAGACTAA (reverse). qPCR was made in presence one-fold *Snp*-buffer, 0.25 mM dNTPs, 0.2 U *Snp*-polymerase (Evrogen, Russia), 0.1-0.4 ng DNA, SYBR Green (1:20000) (Lumiprobe, Russia), 0.5 pmol primers for GAPDH gene. In the case of

telomeric repeats during qPCR, 0.17 pmol Tel1 and 0.5 pmol Tel2 primers were added to the reaction mixture instead of primers for the GAPDH gene. Amplification conditions of telomere regions and the reference gene were different. The polymerase was activated at 95 °C for 3 min. The telomere reaction was immediately subject to 35-40 cycles at 95 °C for 15 s and 54 °C for 2 min. Touchdown PCR was used for the amplification of the reference gene fragment. The primer annealing temperature gradually decreased from 64 to 58 °C for the first seven cycles. One cycle included the following stages: 95 °C for 10 s, 58 °C for 15 s and 72 °C for 15 s. It was repeated 35-40 times. To determine significant differences between telomere length in different age groups, Mann-Whitney U-test was used. T/S values are presented as mean ± SD with 95% CI. CI for means was estimated using the bootstrap method in R version 3.6.2 (Shitikov and Rosenberg, 2013). To estimate differences between samples in percent, we also calculated an inequality between means and 95% CI with the bootstrap method.

3. Results

In the muscle tissue, we analyzed relative telomere length (RTL or T/S) at the final stage of eggs development, in larvae and two-year individuals. The values were 1.01 ± 0.14 (95% CI 0.96 to 1.06), 0.97 ± 0.094 (95% CI 0.932 to 1.003) and 0.91 ± 0.103 (95% CI 0.864 to 0.95), respectively. In fins, RTL was analyzed in larvae and two-year individuals and amounted to 1.06 ± 0.102 (95% CI 1.02 to 1.097) and 0.88 ± 0.092 (95% CI 0.843 to 0.92), respectively. In larvae, RTL was much higher in fins than in muscles (T-test for Dependent Samples: $t = -3.38$, $df = 25$, $p = 0.002$), whereas two-year individuals already had no differences (T-test for Dependent Samples: $t = 0.99$, $df = 21$, $p = 0.333$). Subsequent analysis of the RTL age-related dynamics revealed a significant decrease in tDNA during the early life stage in both tissues (Fig. 1). In this fish, from larvae stage to two-year individuals, RTL decreases by 6% (95% CI 0.7% to 11.6%) in muscles (Mann-Whitney U Test: $U = 218.5$, $Z = 1.99$, $p = 0.046$; $R = -0.32$, $p = 0.024$) and 17.7% (95% CI 12.6% to 23.3%) in fins (Mann-Whitney U Test for fins: $U = 57.5$, $Z = 4.97$, $p = 0.0000$; $R = -0.67$, $p = 0.0000$). Overall, 10.4% (95% CI 3.8% to 16.7%) of tDNA is lost in muscles between the final stage of eggs development and the stage of two-year individuals (Mann-Whitney U Test: $U = 217.5$, $Z = 2.33$, $p = 0.0196$; $R = -0.32$, $p = 0.004$). RTL in muscles and fins of the same individual generally had different values in the stages of larvae and two-year individuals.

4. Discussion and conclusions

In some animals (primates and birds), the length of tDNA and its dynamics are regarded not only as biomarkers of ageing but also biomarkers of experienced stresses (Louzon et al., 2019). For poikilotherms, which include fish, dependence on variable environmental

factors has contributed to the development of protective mechanisms that provide the well-known plasticity of these animals (Woodhead, 1998; Petitjean et al., 2019). Could this lead to the appearance of the same tDNA regulation within this class of vertebrates and, hence, to tDNA dynamics? Analysis of the available data on the tDNA age-related dynamics in fish and its sensitivity to stress allows us to answer in the negative. In the same tissue of different fish species and different tissues of the same fish species, the tDNA dynamics may differ (Table).

In peled, during the early life stages, tDNA decreases in two tissues: muscles and fins (Fig. 1), unlike other members of salmonids, although they have a similar life expectancy (Naslund et al., 2015; Pauliny et al., 2015, see Table). Moreover, close species of salmonids (brown trout and Atlantic salmon) showed an opposite correlation of tDNA length with water temperature. At high temperature, tDNA of *S. trutta* decreased (Debes et al., 2016). On the contrary, growth of *S. salar* during the early stages of ontogeny at different temperatures, including high temperature, led to an increase in tDNA (McLennan et al., 2016; 2018). These data indicate species-specific mechanisms for regulating telomere length under stress conditions as well as a general species-specific dynamics of tDNA during ontogeny.

Different dynamics of tDNA can also be the result of stresses having different effects. Severe stress disables protective systems of an organism, whereas moderate stress mobilizes them (Petitjean et al., 2019). For different species, threshold sensitivity to environmental changes may vary, and protective systems may function differently in different tissues. Cod, *Gadus morhua* Linnaeus 1758, showed most tDNA losses in the liver, a metabolically loaded organ, and insignificant losses in the muscles (de Abechuco et al., 2016). *Danio rerio* had short telomeres in the muscles and the gut, which is likely due to degenerative and inflammatory processes (Carneiro et al., 2016). Thus, the regulation of telomere length occurs differently in the same tissues of different species. Both the functional load of the tissue and a degree of the stress effects during the development of an organism may contribute greatly to this process. Perhaps, regulation of telomere length in peled depends on peculiarities of their growth and development during the early life stages.

Acknowledgments

The authors thank Yu. Bukin for valuable advice. This work was performed at the LIN SB RAS Collective Instrumental Center (<http://www.lin.irk.ru/copp/eng/>) using the unique scientific installation Experimental Freshwater Aquarium Complex for Baikal Hydrobionts at LIN SB RAS supported by RFBR and the Government of the Irkutsk Region, projects Nos. 17-44-388081 r_a and 17-44-388106 r_a, and within the framework of the State Task No. 0345-2019-0002 (AAAA-A16-116122110066-1) "Molecular Ecology and Evolution of Living Systems ...".

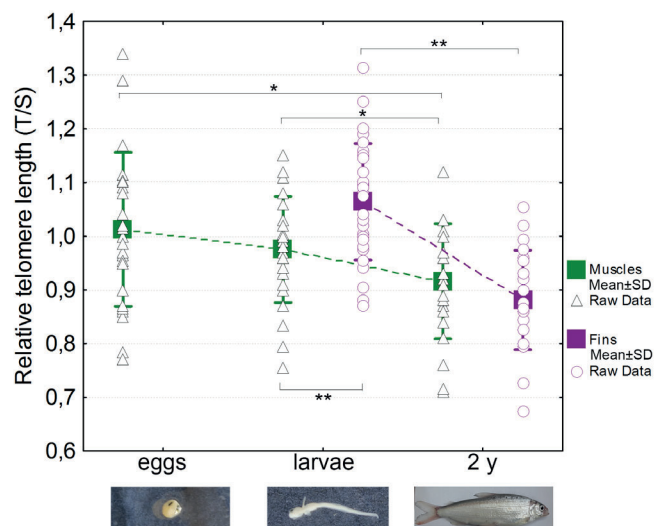


Fig. 1. Age dynamics of tDNA in muscles and fins of peled. It is shown the shortening of telomere length in both tissues. The asterisks denotes a significant difference between the groups (Mann-Whitney U Test): * - $p < 0.05$, ** - $p < 0.005$.

References

- de Abechuco E.L., Hartmann N., Soto M. et al. 2016. Assessing the variability of telomere length measures by means of Telomeric Restriction Fragments (TRF) in different tissues of cod *Gadus morhua*. Gene Reports 5: 117-125. DOI: 10.1016/j.genrep.2016.09.009
- Allsopp R., Vaziri H., Patterson C. et al. 1992. Telomere length predicts replicative capacity of human fibroblasts. Proceedings of the National Academy of Sciences USA 89: 10114-10118. DOI: 10.1073/pnas.89.21.10114
- Caprioli M., Romano M., Romano A. et al. 2013. Nestling telomere length does not predict longevity, but covaries with adult body size in wild barn swallows. Biology Letters 9. DOI: 10.1098/rsbl.2013.0340
- Carneiro M.C., Henriques C.M., Nabais J. et al. 2016. Short telomeres in key tissues initiate local and systemic aging in zebrafish. PLoS Genetics 12. DOI: 10.1371/journal.pgen.1005798
- Cawthon R. 2002. Telomere measurement by quantitative PCR. Nucleic Acids Research 30. DOI: 10.1093/nar/30.10.e47
- Debes P.V., Visse M., Panda B. et al. 2016. Is telomere length a molecular marker of past thermal stress in wild fish? Molecular Ecology 25: 5412-5424. DOI: 10.1111/mec.1385
- Deng Y., Chang S. 2007. Role of telomeres and telomerase in genomic instability, senescence and cancer. Laboratory Investigation 87: 1071-1076. DOI: 10.1038/labinvest.3700673
- Doroshuk N.A., Doroshuk A.D., Rodnenkov O.V. et al. 2013. Change in length of telomeres of the chromosomes under the influence of the climatic conditions that simulate hot weather at Moscow in summer 2010. Kardiologicheskii Vestnik [Cardiological Bulletin] VIII (XX) 2: 32-35. (in Russian)
- Gao J., Munch S.B. 2015. Does reproductive investment decrease telomere length in *Menidia menidia*? PLoS One 10. DOI: 10.1371/journal.pone.0125674
- Gomes N.M., Ryder O.A., Houck M.L. et al. 2011. Comparative biology of mammalian telomeres: hypotheses on ancestral states and the roles of telomeres in longevity determination. Aging Cell 10: 761-768. DOI: 10.1111/j.1474-9726.2011.00718.x
- Greider C.W., Blackburn E.H. 1989. A telomeric

sequence in the RNA of *Tetrahymena* telomerase required for telomere repeat synthesis. *Nature* 337: 331-337. DOI: 10.1038/337331a0

Gruber H., Schaible R., Ridgway I.D. et al. 2014. Telomere-independent ageing in the longest-lived non-colonial animal, *Arctica islandica*. *Experimental Gerontology* 51: 38-45. DOI: 10.1016/j.exger.2013.12.014

Harley C.B., Futcher A.B., Greider C.W. 1990. Telomeres shorten during ageing of human fibroblasts. *Nature* 345: 458-460. DOI: 10.1038/345458a0

Hartmann N., Reichwald K., Lechel A. et al. 2009. Telomeres shorten while Tert expression increases during ageing of the short-lived fish *Nothobranchius furzeri*. *Mechanisms of Ageing and Development* 130: 290-296. DOI: 10.1016/j.mad.2009.01.003

Hatakeyama H., Nakamura K.-I., Izumiyama-Shimomura N. et al. 2008. The teleost *Oryzias latipes* shows telomere shortening with age despite considerable telomerase activity throughout life. *Mechanisms of Ageing and Development* 129: 550-557. DOI: 10.1016/j.mad.2008.05.006

Hayflick L., Moorhead P.S. 1961. The serial cultivation of human diploid cell strains. *Experimental Cell Research* 25: 585-621. DOI: 10.1016/0014-4827(61)90192-6

Hayflick L. 1965. The limited in vitro lifetime of human diploid cell strains. *Experimental Cell Research* 37: 614-636. DOI: 10.1016/0014-4827(65)90211-9

Henriques C.M., Carneiro M.C., Tenente I.M. et al. 2013. Telomerase is required for zebrafish lifespan. *PLoS Genetics* 9. DOI: 10.1371/journal.pgen.1003214

Horn T., Gemmell N.J., Robertson B.C. et al. 2008. Telomere length change in European sea bass (*Dicentrarchus labrax*). *Australian Journal of Zoology* 56: 207-210. DOI: 10.1071/ZO08046

Injaian A.S., Gonzalez-Gomez P.L., Taff C.C. et al. 2019. Traffic noise exposure alters nestling physiology and telomere attrition through direct, but not maternal, effects in a free-living bird. *General and Comparative Endocrinology* 276: 14-21. DOI: 10.1016/j.ygcen.2019.02.017

Izzo C. 2010. Patterns of telomere length change with age in aquatic vertebrates and the phylogenetic distribution of the pattern among jawed vertebrates. PhD Thesis, University Adelaide South Australia, Australia.

Izzo C., Bertozzi T., Gillanders B.M. et al. 2014. Variation in telomere length of the common carp, *Cyprinus carpio* (Cyprinidae), in relation to body length. *Copeia* 1: 87-94. DOI: 10.1643/CI-11-162

Jonsson B., L'Abée-Lund J.H., Heggberget T.G. et al. 1991. Longevity, body size, and growth in anadromous brown trout (*Salmo trutta*). *Canadian Journal of Fisheries and Aquatic Sciences* 48: 1838-1845. DOI: 10.1139/f91-217

de Lange T. 2005. Shelterin: the protein complex that shapes and safeguards human telomeres. *Genes Development* 19: 2100-2110. DOI: 10.1101/gad.1346005

López-Otín C., Blasco M.A., Partridge L. et al. 2013. The hallmarks of aging. *Cell* 153: 1194-1217. DOI: 10.1016/j.cell.2013.05.039

Louzon M., Coeurdassier M., Gimbert F. et al. 2019. Telomere dynamic in humans and animals: review and perspectives in environmental toxicology. *Environment International* 131. DOI: 10.1016/j.envint.2019.105025

Maximova N., Koroleva A., Sitnikova T. et al. 2017. Age dynamics of telomere length of Baikal gastropods is sex specific and multidirectional. *Folia Biologica (Krakow)* 65: 187-197. DOI: 10.3409/fb65_4.187

Meyne J., Ratliff R.L., Moyzis R.K. 1989. Conservation of the human telomere sequence (TTAGGG)_n among vertebrates. *Proceedings of the National Academy of Sciences USA* 86: 7049-7053. DOI: 10.1073/pnas.86.18.7049

McLennan D., Armstrong J.D., Stewart D.C. et al.

2016. Interactions between parental traits, environmental harshness and growth rate in determining telomere length in wild juvenile salmon. *Molecular Ecology* 25: 5425-5438. DOI: 10.1111/mec.13857

McLennan D., Armstrong J.D., Stewart D.C. et al. 2018. Telomere elongation during early development is independent of environmental temperatures in Atlantic salmon. *Journal of Experimental Biology* 221. DOI: 10.1242/jeb.178616

Mukhachev I.S. 2003. Biotechnics of faster breeding of marketable peled. Tyumen: FGU IPP Tyumen. (in Russian)

Naslund J., Pauliny A., Blomqvist D. et al. 2015. Telomere dynamics in wild brown trout: effects of compensatory growth and early growth investment. *Oecologia* 177: 1221-1230. DOI: 10.1007/s00442-015-3263-0

Oikawa S., Tada-Oikawa S., Kawanishi S. 2001. Site-specific DNA damage at the GGG sequence by UVA involves acceleration of telomere shortening. *Biochemistry* 40: 4763-4768. DOI: 10.1021/bi002721g

Olovnikov A.M. 1971. Principles of marginotomy in template synthesis of polynucleotides. *Doklady Akademii Nauk SSSR [Reports of the USSR Academy of Sciences]* 201: 1496-1499. (in Russian)

Olovnikov A.M. 1973. A theory of marginotomy. The incomplete copying of template margin in enzymic synthesis of polynucleotides and biological significance of the phenomenon. *Journal of Theoretical Biology* 41: 181-190. DOI: 10.1016/0022-5193(73)90198-7

Paizt R.T., Haussmann M.F., Bowden R.M. et al. 2004. Long telomeres may minimize the effect of aging in the Painted Turtle. *Integrative and Comparative Biology* 44: 617.

Pauliny A., Devlin R.H., Johnsson J.I. et al. 2015. Rapid growth accelerates telomere attrition in a transgenic fish. *BMC Evolutionary Biology* 15: 159. DOI: 10.1186/s12862-015-0436-8

Petitjean Q., Jean S., Gandar A. et al. 2019. Stress responses in fish: from molecular to evolutionary processes. *Science of the Total Environment* 684: 371-380. DOI: 10.1016/j.scitotenv.2019.05.357

Rollings N., Miller E., Olsson M. 2014. Telomeric attrition with age and temperature in Eastern mosquitofish (*Gambusia holbrooki*). *Naturwissenschaften [Natural Sciences]* 101: 241-244. DOI: 10.1007/s00114-014-1142-x

Romanuk A., Paszel-Jaworska A., Totoń E. et al. 2019. The non-canonical functions of telomerase: to turn off or not to turn off. *Molecular Biology Reports* 46: 1401-1411. DOI: 10.1007/s11033-018-4496-x

Sambrook J., Fritsch E., Maniatis T. 1989. *Molecular cloning: a laboratory manual*. New York: Cold Spring Harbor.

Shitikov V.K., Rosenberg G.S. 2013. Randomization and bootstrap: statistical analysis in biology and ecology using R. Tol'yatti: Cassandra. (in Russian)

Simide R., Angelier F., Gaillard S. et al. 2016. Age and heat stress as determinants of telomere length in a long-lived fish, the Siberian sturgeon. *Physiological and Biochemical Zoology* 89: 441-447. DOI: 10.1086/687378























Singh A., Kukreti R., Saso L. et al. 2019. Oxidative stress: role and response of short guanine tracts at genomic locations. *The International Journal of Molecular Sciences* 20. DOI: 10.3390/ijms20174258





Tsui J.C.Y. 2005. Evaluation of telomere length as an age marker in marine teleost. PhD Thesis, University of Hong Kong, China.

Voropaeva E.N., Maksimov V.N., Malyutina S.K. et al. 2015. Effects of DNA quality on the measurement of telomere length. *Molecular Biology (Mosk)* 49: 571-576. DOI: 10.7868/S0026898415040199

Woodhead A.D. 1998. Aging, the fishy side: an appreciation of Alex Comfort's studies. *Experimental Gerontology* 33: 39-51. DOI: 10.1016/s0531-5565(97)00064-8

Table. Age telomere length dynamics in different species of fish, their appearance and lifespan

Species, common name	Appearance	ML ¹	TL dynamics		Reference
			muscle	fin	
Chondrichthyes (cartilaginous fish)					
<i>Heterodontus portusjacksoni</i> , Port Jackson shark		35 y	↔	↔	Izzo, 2010
<i>Squalus megalops</i> , Piked spurdog		75 y	↔		Izzo, 2010
<i>Urolophus paucimaculatus</i> , Sparsely spotted stingray		12 y	↔		Izzo, 2010
<i>Dentiraja lemprieri</i> , Thornback skate		12 y	↔		Izzo, 2010
<i>Trygonorrhina dumerilii</i> , Southern fiddler ray		15 y	↔		Izzo, 2010
<i>Callorhinchus milii</i> , elephant shark		6 y	↔		Izzo, 2010
Osteichthyes (bony fish)					
<i>Chrysophys aurutus</i> , Snapper		35 y	↓		Izzo, 2010
<i>Cyprinus carpio</i> , Common carp		11 y	↑	↔	Izzo et al., 2014
<i>Lutjanus argentimaculatus</i> , Mangrove red snapper		7 y	↓		Tsui, 2005
<i>Macquaria ambigua</i> , Golden perch		20 y	↔		Izzo, 2010
<i>Menidia menidia</i> , Atlantic silverside		2 y	↔		Gao and Munch, 2015
<i>Neoceratodus forsteri</i> , Australian lungfish		65 y	↔		Izzo, 2010
<i>Nothobranchius furzeri</i> (GRZ), Turquoise killifish		3.5 mo	↔		Hartmann et al., 2009
<i>Nothobranchius furzeri</i> (MZM-0403)		6 mo	↓		Hartmann et al., 2009
<i>Oryzias latipes</i> , Medaka, Japanese rice fish		5 y	↓		Hatakeyama et al., 2008
<i>Platycephalus bassensis</i> , Sand flathead		23 y	↓		Izzo, 2010
<i>Pseudocaranx wrighti</i> , Silver trevally		13 y	↔		Izzo, 2010
<i>Thamnaconus degeni</i> , Degen's (bluefin) leatherjacket		18 y	↓		Izzo, 2010
<i>Trachurus novaezelandiae</i> , Southern yellowtail scad		25 y	↔		Izzo, 2010
<i>Upeneichthys vlamingii</i> , Southern goatfish		10 y	↓		Izzo, 2010
<i>Gadus morhua</i> , Atlantic cod		25 y	↔		de Abechuco et al., 2016
<i>Gambusia holbrooki</i> , Eastern mosquitofish		3 y	↓		Rollings et al., 2014
<i>Danio rerio</i> , Zebra-fish		5.5 y		↓	Henriques et al., 2013

<i>Acipenser baerii</i> , Siberian sturgeon		60 y		↓	Simide et al., 2016
<i>Salmo trutta</i> , Atlantic brown salmon, trout		11 y		↔	Naslund et al., 2015
<i>Oncorhynchus kisutch</i> , Coho salmon		5 y		↔	Pauliny et al., 2015
<i>Coregonus peled</i> , Peled		12 y	↓	↓	This study

¹ – Maximum lifespan, sometimes it depends on the population (for example, the lifespan of *Salmo trutta* can vary from 4 to 11 years (Jonsson et al., 1991)). Arrows describe telomere shortening (↓), maintenance (↔), or increasing (↑) with age. Some data for the table were taken from E.I. de Abechuco et al., 2016 and R. Simide et al., 2016.

Chemical composition and quality of water of the Selenga River and its tributaries in Mongolia

Sorokovikova L.M.¹, Tomberg I.V.^{1,*}, Stepanova O.G.¹, Marinaite I.I.¹,
Bashenkaeva N.V.¹, Khash-Erdene S.², Fedotov A.P.¹

¹ Limnological Institute, Siberian Branch of the Russian Academy of Sciences, Ulan-Batorskaya Str., 3, Irkutsk, 664033, Russia

² Mongolian Knowledge Society, kampus Margad, Erdenet 61000, Mongolia

The chemical composition and current state of water quality of the Selenga River and its tributaries in Mongolia are considered in this article based on the hydrochemical studies carried out in July 2013-2014. The observed changes in the chemical composition of the water resulted from natural and anthropogenic factors are analyzed. It is shown that water quality of the Selenga River and its tributaries worsened because of the entering of polluting components from the catchment area of Ulaanbaatar city and its wastewater. No influence of the wastewater from the Erdenet Ore-Dressing Plant (EODP) on the trace elements content in the water of the Orkhon and Selenga Rivers is revealed.

Keywords: chemical composition, water quality, nutrients, petrochemicals, polycyclic aromatic hydrocarbons, trace elements

1. Introduction

The Selenga River is the main tributary of Lake Baikal, flowing through the territories of Mongolia and Russia. The length of the river is 1024 km; from its total length, the Selenga flows for 615 km in the territory of Mongolia. Intensive development of natural resources in Mongolia, growth of industry and agriculture increased anthropogenic load on the catchment area of the Selenga River and worsened the quality of its water (Anikanova et al., 1991; Tulokhonov et al., 2009). For example, the world's largest copper-molybdenum deposit being developed by the Erdenet Ore-Dressing Plant and a great number of illicit gold mining sites are located in the watershed of the Selenga River.

As a result, in recent decades, at the boundary with Mongolia, the disorders of the chemical composition of the Selenga River water have been observed; the concentrations of sulphates, nutrients and other components have increased. At the end of the 1990s, the chemical composition of the water was similar to the natural background. For example, sulphate concentrations during the period of open riverbed near the Naushki settlement ranged from 7.5 to 8.5 mg/l (Sorokovikova et al., 2013), while sulphate concentrations continued increasing up to 17.23 mg/l in July, 2018 and up to 20.3 mg/l in 2019. The data obtained during complex international monitoring and the data from the Ministry of Natural Resources of Mongolia (Dolgorsvuren et al., 2012) indicate the

increase of the concentrations of sulphates, heavy metals and nutrients in the Selenga River and its tributaries in the territory of Mongolia.

The aim of this work is to investigate the water chemistry of the Selenga River and its major tributaries, and to assess current water quality status.

2. Materials and methods

The samples of the water were collected from 20 river stations in July, 2013-2014 (Fig. 1). The samples for chemical analysis were filtered through a membrane filter with a pore size of 0.45 µm. The determination of cations was carried out using the atomic-absorption spectrometry method whose relative error in the determination was 2-3% (Rukovodstvo..., 2009); the determination of anions was carried out using the microcolumn high performance liquid chromatography (HPLC) method. The relative error in the determination of anions by the method did not exceed 5-10% (Baram et al., 1999). The determination of inorganic phosphorus was carried out using the colorimetric method with ammonium molybdate; its relative error was 1.5%. The determination of ammonium nitrogen was carried out using the indophenol method; the relative error was 4-5%. The organic matter content was determined using the dichromate method (Wetzel and Likens, 2003; Rukovodstvo..., 2009). Measured concentrations of the major ions were controlled by the calculating of the error of ionic balance (R_1) and the error of the comparison

*Corresponding author.

E-mail address: kaktus@lin.irk.ru (I.V. Tomberg)

of the calculated and measured specific electrical conductivity (R_2). The reliability of the obtained results on the concentrations of nutrients was verified by the regular quality control of the analyses within the framework of the EANET international program on the “surface waters” standard samples testing. The concentrations of polycyclic aromatic hydrocarbons (PAH) were measured using chromatography mass spectrometry (Gorshkov et al., 2004). Quantification of individual PAHs (phenanthrene-d10, chrysene-d12 and perylene-l12) was done using “Supelco” standards (USA). The error of the measurements did not exceed 10%. The samples for multielement analysis by ICP-MS were in situ filtered through a membrane filter with a pore size of 0.45 μm . The samples were analyzed using quadrupole mass spectrometer Agilent 7500e.

3. Results and discussion

3.1. Ion composition of water

The chemical composition of the Selenga River over the entire territory of its basin is formed under similar geological and climatic conditions that could explain its low variability along the river. The Selenga River waters and its tributaries along the entire length are characterized as being a hydro-carbonate calcium type. It was found out that the total content of the major ions in the Selenga River increased from 199.8 to 237.4 mg/l in the upper reaches of the river (between the stations 1 and 2) (Fig. 2). However, the concentrations of ions decreased to 206.9 mg/l (the Naushki settlement,

Russian-Mongolian boundary) due to the dissolving of the Selenga River by the tributaries. In the tributaries of the Selenga River the highest content of ions was observed in the Khainun River (Table 1), however, this river did not significantly affect the chemical composition of the Selenga River water (Fig. 2) due to its low water budget. The obtained data showed that the Orkhon River mostly influenced the Selenga River water quality.

The study of the Orkhon River carried out in July 2014 showed that the total content of the major ions in the water ranged from 131.3 to 163.3 mg/l. The concentrations of ions in the Orkhon tributaries varied by an order or more (Table 1). Thus, the highest concentrations of ions and their sum were observed in the Burgalta and Khangal Rivers (Table 1). As a result, the highest content of ions is observed downstream of the inflow point of the Burgalta and Khangal Rivers. This fact could be related to the effect made by the wastewater from the Erdenet Ore-Dressing Plant.

However, most ecological problems are determined in the Tuul River below Ulaanbaatar. For example, the sum of ions and chlorine-ions increases 2 and 14 times, respectively, in comparison to their concentrations in the river reaches above the city (Table 1).

The inflow of the low mineralized water of the Eroo River causes the decrease of the sum of ions and sulphates in the Orkhon River. Despite the fact that the inflow of the Orkhon River increases the concentrations of sulphates, chlorides and sodium in the Selenga River.



Fig. 1. Map of the sampling locations in 2013-2014.

1 – the Selenga River downstream of the confluence point of the Ider and Muren Rivers; 2 – the Selenga River upstream of the Khanuun River; 3 – the Khanuun River; 4 – the Selenga River upstream of the Egyin River; 5 – the Egyin River; 6 – the Selenga River downstream of the Egyin River; 7 – the Selenga River upstream of the Orkhon River; 8 – the Eroo River; 9 – the Tuul river upstream from Ulaanbaatar; 10 – the Tuul River downstream from Ulaanbaatar; 11 – the Orkhon River upstream from the Bulgan settlement; 12 – the Orkhon River downstream from the Bulgan settlement; 13 – the Khangal River; 14 – the Burgalta River; 15 – the Borun-Buren River; 16 – the Orkhon River downstream of the Kharaa River; 17 – the Kharaa River; 18 – the Orkhon River downstream of the Eroo River; 19 – the Orkhon River downstream of the Eroo River; 20 – the Selenga River (Naushki).

Table 1. The sum of ions and the concentration of major ions (mg/l) in the tributaries of the Selenga River in the territory of Mongolia. Numbers of sampling stations are shown according to Fig. 1

Sampling location	Sum of ions	Na ⁺	K ⁺	Ca ²⁺	Mg ²⁺	Cl ⁻	SO ₄ ²⁻	HCO ₃ ⁻
Tributaries of the Selenga River, 2013								
3 (the Khanuin River)	318.6	27.2	1.9	32.7	15.0	3.6	19.9	218.4
5 (the Egyin River)	200.0	3.9	1.4	34.4	7.4	0.63	16.3	136.0
19 (the Orkhon River)	188.6	11.7	1.8	25.9	6.9	5.1	16.4	120.8
Tributaries of the Orkhon River, 2014								
9 (the Tuul River)	47.6	2.1	0.76	8.2	1.1	0.3	4.6	30.5
10 (the Tuul River)	93.3	6.5	1.68	14.2	2.2	4.4	10.6	53.7
13 (the Khangal River)	808.2	55.0	7.90	103.0	36.0	37.2	272.7	296.5
14 (the Burgalta River)	714.3	52.1	4.63	101.6	32.0	26.0	242.9	255.0
15 (the Borun-Buren River)	235.1	9.8	1.23	36.0	10.0	1.5	10.6	165.9
17 (the Kharaa River)	215.2	12.5	1.99	30.6	8.8	4.6	18.9	137.9
8 (the Eroo River)	93.6	3.7	1.2	14.7	3.0	0.67	6.2	64.1
MAC level for drinking water	1000	200	-	-	-	350	500	-
MNS 4586-98						300	100	

3.2. Nutrients and organic matter

Nutrient concentrations in the studied rivers ranged widely. The content of ammonium nitrogen along the Selenga and Orkhon Rivers was almost equal in both rivers and ranged from 0.01mg to 0.03 mg N/l. The concentrations of nitrate nitrogen differed considerably; in the Selenga River, the concentrations ranged from 0.04 to 0.13 mg N/l, in the Orkhon River – from 0.23 to 0.48 mg N/l, reaching their maximum values downstream of the inflow of the Kharaa River. The concentration of nitrite nitrogen in these rivers did not exceed 0.003 mg N/l. In July 2013-2014, the total of mineral nitrogen in the Selenga River did not exceed 0.14 mg N/l before the inflow point of the Orkhon River, and was 0.13 mg N/l below the confluence (the Naushki settlement).

In the water of the tributaries, the concentrations of nitrogen considerably exceed those of the Selenga and Orkhon Rivers. The highest values are observed in the Khangal, Burgalta and Tuul Rivers downstream from Ulaanbaatar (Table 2). It could be related to the influence of agricultural fields and livestock farms due to the presence of high concentrations of nitrite nitrogen.

During the observation period, the concentrations of mineral phosphorus were 7-8 µg P/l in the upper reaches of the Selenga River (between the stations 1 and 2), while total phosphorus was 162-170 µg P/l (Table 2, Fig. 3a). We suppose it is due to the intensive agricultural development, including livestock farms, and due to the entering of phosphorus from the catchment area. Downstream the Selenga River, within the Mongolian section, the content of total phosphorus decreases and does not exceed 92 µg P/l, the content of mineral phosphorus does not exceed 10 µg P/l.

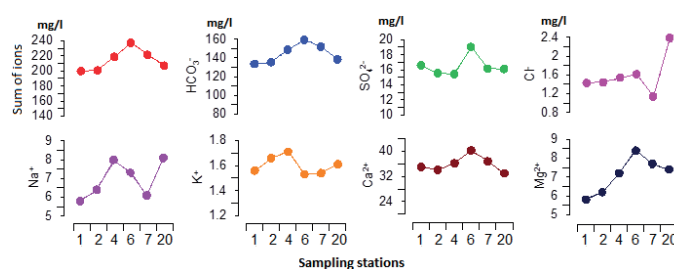
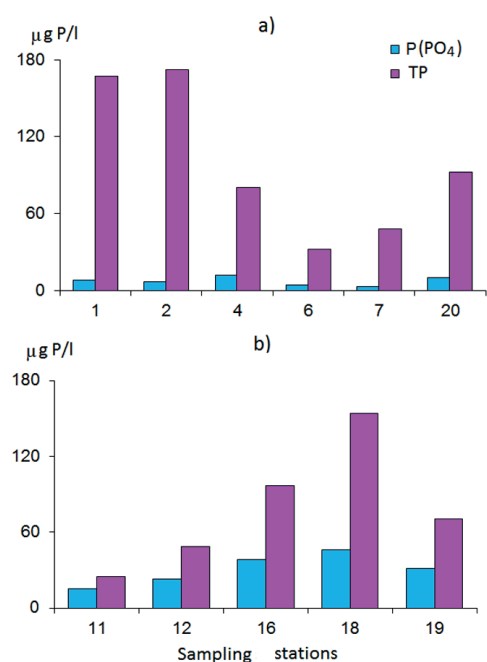
**Fig. 2.** Spatial dynamics of the concentrations of major ions in the Selenga River and its tributaries, 2013. Numbers of sampling stations are shown according to Fig. 1**Fig. 3.** Changes of the concentrations of phosphate (1) and total phosphorus (2) in the Selenga (a) and Orkhon (b) Rivers. Numbers of sampling stations are shown according to Fig. 1

Table 2. The dynamics of the nutrient concentrations in the tributaries of the Selenga and Orkhon Rivers, July 2013-2014. Numbers of sampling stations are shown according to Fig. 1

Sampling location	NH ₄ ⁺	NO ₂ ⁻	NO ₃ ⁻	P _{min.}	P _{tot.}	C _{org.}
	mg N/l			µg P/l		mg C/l
The Selenga River, 2013						
1	0.03	0.002	0.09	8	162	2.6
2	0.01	0.002	0.13	7	172	2.4
4	0.01	0.002	0.10	12	80	2.8
6	0.01	0.001	0.11	4	32	4.1
7	<dl	0.002	0.04	3	48	3.6
20	<dl	0.002	0.10	10	92	3.6
Tributaries of the Selenga River, 2013						
3 (the Khainun River)	0.01	0.001	0.03	6	35	3.0
5 (the Egyin River)	0.01	0.001	0.06	2	8	4.1
19 (the Orkhon River)	<dl	0.002	0.27	43	212	5.3
The Selenga River, 2014						
7	0.02	0.003	0.12	12	17	6.8
20	0.02	0.002	0.11	6	82	5.9
The Orkhon River, 2014						
11	0.02	0.002	0.24	15	71	13.6
12	0.03	0.003	0.23	23	82	5.1
16	0.02	0.002	0.43	38	147	14.2
18	0.03	0.002	0.48	46	154	6.0
19	0.03	0.002	0.33	31	77	6.3
Tributaries of the Orkhon River, 2014						
9 (the Tuul River)	0.02	0.002	0.06	<dl	32	6.3
10 (the Tuul River)	0.20	0.050	0.40	72	101	11.4
13 (the Khangal River)	0.15	2.557	10.02	26	209	4.9
14 (the Burgalta River)	0.00	0.129	5.52	161	163	5.1
15 (the Borun-Buren River)	0.03	0.002	0.05	26	32	4.3
17 (the Kharaa River)	0.03	0.003	0.40	38	-	6.5
8 (the Eroo River)	0.03	0.002	0.05	1	15	8.2
MNS 4586-98	-	-	-	-	100	-

dl – detection limit

In some tributaries, the concentrations of both mineral and total phosphorus are considerably higher than those are in the Orkhon River (Table 2). It is supposed to be related to the intensive anthropogenic load on their catchment areas and to the low water level. The highest phosphorus concentrations are observed in the Orkhon River tributaries, the Burgalta, Khangal and Tuul Rivers, downstream from Ulaanbaatar. The lowest concentrations were in the Tuul River upstream from Ulaanbaatar and the Eroo River.

Tributaries water inflows, enriched with phosphorus species, result the increase of the concentrations in the Orkhon River. The spatial variations of the concentrations of mineral and total phosphorus in the Orkhon River are shown in Fig. 3b. As can be seen in the figure, from the upper reaches to the mouth of the Orkhon River, the phosphorus concentrations gradually increase and then decrease downstream of the inflow of the Eroo River. The

phosphorus concentration in the Selenga River varies depending on the total phosphorus content in the upper reaches of the Orkhon River. Thus, in the Orkhon River, it was 212 µg P/l, in the Selenga River near the Naushki settlement, it was 92 µg P/l in 2013 (Table 2).

According to the Mongolian water quality standards (Mongol ulsyn snadart, 1999), the content of phosphorus in water should not exceed 100 µg P/l. As can be seen from the obtained data on the Burgalta, Khangal and Tuul Rivers, the content of phosphorus exceeds the maximum allowable concentrations.

The content of organic carbon in the rivers ranged from 2.4 to 14.2 mg C/l. The increased content of organic matter was reported below the inflow of the Tuul River downstream from Ulaanbaatar (Table 2). The increase of the concentrations of organic carbon in the Tuul River in the reach downstream from Ulaanbaatar points to the intensive anthropogenic load on the river's ecosystem and to the low water quality.

3.3. Petrochemicals and polycyclic aromatic hydrocarbons (PAHs)

The content of petrochemicals in the Orkhon River along its entire length and in its tributaries was low, < 0.005 - 0.017 mg/l (Table 3). The concentrations were slightly increased in the Tuul River downstream from Ulaanbaatar and in the Khangal River downstream from the Ore-Dressing Plant.

PAHs are important water quality indicators, classified as persistent organic pollutants having mutagenic and cancerogenic characteristics (Menzie and Potokib, 1992). The content of the sum of sixteen PAHs in the Orkhon River ranged from 6.5 to 34 ng/l (Table 4). The increased content of PAHs was observed in the Tuul (downstream from Ulaanbaatar) and Khangal Rivers. So-called "light" PAHs (naphthalene, acenaphthylene, fluorine, phenanthrene, anthracene, fluoranthene) make the major contribution to the sum of PAHs. The concentrations of the "heavy" PAHs (benz[a]anthracene, chrysene, benz[b]fluoranthene, benz[k]fluoranthene, benz[a]pyrene, indeno[1,2,3-c,d]pyrene, benz[g,h,i]perylene, bibenz[a,h]anthracene) are found out at the sensitivity level of the used method. The concentrations of benz[a]pyrene and naphthalene were lower than the ones regulated by the Russian state standards for drinking and natural waters (Prikaz..., 2018; SanPin 2.1.4.1074-01, 2018).

For instance, European Environmental Agency monitors the total content of six PAHs (benz[a]pyrene, benz[b]fluoranthene, benz[k]fluoranthene, benz[g,h,i]perylene, indeno[1,2,3-c,d]pyrene) and their total concentration in drinking water should not exceed 110 ng/l (Council directive, 1998). The concentration of the six PAHs in the Selenga River also was < 200 ng/l.

In general, the concentrations of the sum of PAHs in the Orkhon River were low. For example, the sums of PAHs were 910-1520 ng/l in the Aodjang River (China) (Li et al., 2010), 4.2 -310 ng/l in the Olkha River (East Siberia, Russia) (Marinaite et al., 2013), and 78 -159 ng/l in the delta of the Selenga River in spring (Marinaite, 2010).

Table 3. The content of petrochemicals (mg/l) in the Orkhon River and its tributaries in the territory of Mongolia, July 2014. Numbers of sampling stations are shown according to Fig. 1.

Sampling stations	C, mg/l
7	0.007
8	0.006
9	0.007
10	0.011
11	< dl
12	0.006
13	0.017
14	0.008
15	0.005
16	0.005
17	0.006
18	0.005
19	0.006
20	0.008

dl – detection limit

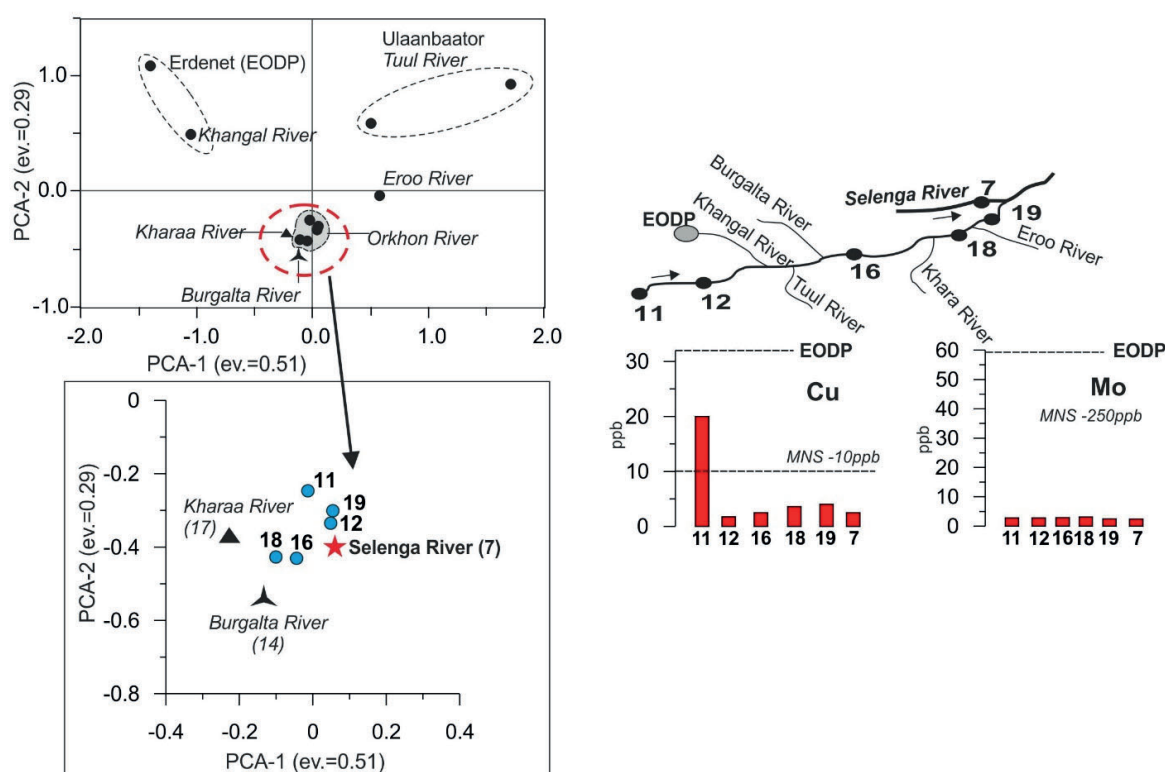


Fig. 4. Trace elements areas of the studied watershed of the Orkhon River based on PCA.

Table 4. The content of PAHs (ng/l) in the Orkhon River and its tributaries and in The Selenga River. July 2014. Numbers of sampling stations are shown according to Fig. 1.

Components	Sampling stations													
	7	8	9	10	11	12	13	14	15	16	17	18	19	20
Naphtalene	4.1	3.5	3.3	4.5	2.3	5.3	9.3	4.3	4.1	5.4	3.2	3.6	3.9	6.2
Acenaphthylene	<dl	<dl	<dl	<dl	<dl	<dl	<dl	<dl	<dl	<dl	<dl	<dl	<dl	<dl
Acenaphthene	<dl	<dl	<dl	<dl	<dl	<dl	<dl	<dl	<dl	<dl	<dl	<dl	<dl	<dl
Fluorene	0.6	0.5	0.4	<dl	0.5	0.9	<dl	2.1	2.1	0.6	0.7	0.4	0.5	0.9
Phenanthrene	1.9	1.6	1.5	12	0.6	2.1	17	2	1.9	2.7	2.0	1.7	1.7	2.5
Anthracene	<dl	<dl	<dl	<dl	<dl	<dl	<dl	<dl	<dl	<dl	<dl	<dl	<dl	<dl
Fluoranthene	0.5	0.5	0.6	2.5	0.2	0.7	3.7	0.6	0.6	0.3	0.5	0.4	0.5	0.7
Pyrene	0.7	0.7	0.8	3.7	0.3	0.8	3.5	0.7	0.5	0.3	0.6	0.6	0.7	0.9
Sum of PAHs	7.8	6.8	6.5	23	3.9	10	34	10	9.2	9.3	7.0	6.7	7.3	11

dl – detection limit

3.4. Trace elements in water

The trace element composition of the studied watershed of the Orkhon River can be divided into three areas by Principal component analysis (PCA) (Fig. 4). The first area – the Tuul River near Ulaanbaatar, the second area – the area near the EODP and the Khangal River, and the third area includes the Orkhon, Selenga, Kharaa and Burgalta Rivers. In wastewaters from the sludge storage pits of the EODP, the concentrations of copper and molybdenum exceeded the MAC level set by the Russian and Mongolian standards for natural waters. However, 70 km downstream the Orkhon River from the EODP, the concentrations of copper and molybdenum in the river were close to the values characteristic for the upper reaches of the Orkhon River. In addition, the microelement composition of the Selenga River before the confluence with the Orkhon River is similar to the microelement composition in the lower reaches of the Orkhon River (Fig. 4).

While the microelement content of the Eroo River differs from the content of other tributaries of the Orkhon River, it was not found out that the Ore-Processing Mill of Darkhan affected the microelement composition of the Eroo and Orkhon Rivers. In general, it is most likely that there was no significant influence of these tributaries on the elemental composition of the Orkhon River.

4. Conclusions

The chemical composition of the Selenga River and its tributaries was studied in 2013-2014. It was found out that the concentrations of sulphate increased up to 16-16 mg/l as compared with the beginning of the 2000s. As can be seen from the obtained data, the content of phosphorus in the Burgalta, Khangal and Tuul Rivers exceeds the maximum allowable concentrations set by the Mongolian water quality standards. On the contrary, the content of total phosphorus in the Selenga River at the site the Khanuin River – Naushki did not exceed the maximum allowable concentrations. The concentrations of benz[a]pyrene and naphthalene were

lower than the ones set by the Russian state standards for drinking and natural waters. The elemental composition of the studied rivers is quite similar within the inter-annual aspect. It was not found out that the EDOP and the Ore-Processing Mill of Darkhan affected the microelement composition of the Orkhon and Eroo Rivers.

References

- Anikanova M.N., Batima P., Nyamzhav P. et al. 1991. O raschete stoka khimicheskikh veshchestv s vodami rek basseyna r. Selengi na territorii MNR. In: Izrael Yu.A., Anokhin Yu.A. (Eds.), Monitoring sostoyaniya ozera Baykal. Leningrad, pp. 63-68. (in Russian)
- Baram G.I., Vereshchagin A.L., Golobokova L.P. 1999. Microcolumn high performance liquid chromatography with UV detection for the determination of anions in environmental materials. *Journal of Analytical Chemistry* 54: 962-965. (in Russian)
- Council directive 98/83/EC. 1998. On the quality of water intended for human consumption.
- Dolgorsvuren G., Bron J., van der Linden W. 2012. Integrated water management national assessment report. Volume I. Ulaanbaatar: Ministry of Environment and Green Development. (in Mongolian)
- Gorshkov A.G., Marinaite I.I., Zhamsueva G.S. et al. 2004. Benzopyrene isomer ratio in organic reaction of aerosols over water surface of Lake Baikal. *Journal of Aerosol Science* 35: 1059-1060. DOI:10.1016/S0021-8502(19)30264-2
- Li J., Shang X., Zhao Z. et al. 2010. Polycyclic aromatic hydrocarbons in water, sediment, soil, and plants of the Aojiang River waterway in Wenzhou, China. *Hazardous Materials* 173: 75-81. DOI: 10.1016/j.jhazmat.2009.08.050
- Marinaite I.I. Polycyclic aromatic hydrocarbons in the snow cover and water of the Selenga River. 2010. In: International Conference "Deltas of Eurasia: Origin, Evolution, Ecology, and Economic Development", pp. 140-144. (in Russian)
- Marinaite I.I., Gorshkov A.G., Taranenko E.N. et al. 2013. Distribution of polycyclic aromatic hydrocarbons in natural objects over the territory of scattering the emissions from the Irkutsk aluminum plant (Shelekhov city, the Irkutsk region). *Chemistry for Sustainable Development* 21: 135-146.
- Menzie C.A., Potokib B. 1992. Exposure to carcinogenic PAHs in the environment. *Environmental Science and Technology* 26: 1278-1284. DOI: 10.1021/es00031a002
- Mongol ulsyn standartrt. 1999. (in Mongolian)

Prikaz Minsel'khoza RF No. 552 (Izmeneniya ot 12.10.2018). 2016. On the approval of water quality standards for water bodies used for fishery, including standards for maximum allowable concentrations of hazardous substances in water of water bodies used for fishery. (in Russian)

Rukovodstvo po khimicheskomu analizu poverkhnostnykh vod sushi. 2009. In: Boeva L.V. (Ed.). Leningrad: Gidrometeoizdat. (in Russian)

SanPiN 2.1.4.1074-01. 2018. Drinking water. Hygienic requirements for water quality of centralized drinking water supply systems. Quality control. Hygienic requirements for provision of safety of hot water supply systems. (in Russian)

Sorokovikova L.M., Popovskaya G.I., Tomberg I.V. et al. 2013. The Selenga river water quality on the border

with Mongolia at the beginning of the 21st century. *Russian Meteorology and Hydrology* 2: 126-133. DOI: 10.3103/S106837391302010611.

Sorokovikova L.M., Sinukovich V.N., Golobokova L.P. et al. 2000. Selenga ion runoff formation under present-day conditions. *Vodnye Resursy* 5: 560-565. (in Russian)

Tulokhonov A.K., Enkhtsetseg B., Shekhovtsov A.A. et al. 2009. Transgranichnyy diagnosticheskiy analiz ekologo-ekonomicheskikh problem. In: Baykal'skaya Aziya: ekonomika, ekologiya, ustoychivoye razvitiye (rezul'taty mezhdunarodnogo sotrudnichestva): kollektivnaya monografiya. Ulan-Ude, pp. 30-32. (in Russian)

Wetzel R.G., Likens G.E. 1991. *Limnological Analyses*. New York: Springer Verlag.

Different rates of molecular evolution of mitochondrial genes in Baikalian and non-Baikalian amphipods

Romanova E.V.¹, Sherbakov D.Y.^{1,2*}¹ Limnological Institute, Siberian Branch of the Russian Academy of Sciences, Ulan-Batorskaya Str., 3, Irkutsk, 664033, Russia² Irkutsk State University, Karl Marx Str., 1, Irkutsk, 664003, Russia

ABSTRACT. Rates of molecular evolution in eight protein-coding mitochondrial genes from two parallel lineages of Baikalian amphipods were compared to those in the representatives of gen. *Gammarus*. In six genes (Atp6, Cox2, Cox3, Nad1, Nad5, Nad6), there was a significant acceleration in the evolutionary rate of Baikalian species over those from *Gammarus* group. Correlation of the absolute rate of base substitution accumulation and the acceleration was insignificant, that allowed us to propose mostly adaptive reasons for the effect found.

Keywords: Rate of evolution, mitogenome, genetic distances, Baikal

1. Introduction

The accumulation rate of base substitutions (rate of molecular evolution) depends on various factors, including physiological characteristics, environmental conditions and life history of species (Fazalova et al., 2010; Ellegren and Galtier, 2016). Therefore, significant changes in the rate of molecular evolution in sister groups may provide valuable insight into driving forces of adaptive radiation and speciation. In particular, some studies showed a positive correlation between the rate of molecular evolution and the rate of species diversification (Lanfear et al., 2010; Bromham et al., 2013).

One of the most attractive and mysterious cases of a wide variation of diversification rates is the adaptive radiation of amphipods in Lake Baikal where they evolved into two very diverse species flocks. These flocks result from two independent introductions of the gen. *Gammarus* representatives into the lake (Macdonald et al., 2005; Hou and Sket, 2016; Naumenko et al., 2017). Since the species of gen. *Gammarus* are very uniform morphologically (Pinkster, 1983), the adaptive radiations of the *Gammarus* descendants in Lake Baikal led to the appearance of two very diverse morphologically and ecologically amphipod lineages (Kamaltynov, 2009).

This peculiar evolutionary background makes it possible to test the hypothesis, according to which an acceleration of speciation and morphological diversification is accompanied by an acceleration of the rate at which base substitutions are fixed in genomes (Rabosky, 2019; Wiens and Scholl, 2019).

Several mitochondrial genomes (mitogenomes) have been sequenced recently from the representatives of both Baikalian species and several species of gen. *Gammarus* (Krebes and Bastrop, 2012; Romanova et al., 2016; Macher et al., 2017; Cormier et al., 2018; Sun et al., 2020). Since the proteins coded in mitochondrial DNA are not directly involved in morphogenesis, the deviations in the rate of their molecular evolution may serve as an indication of changes in the average rate of molecular evolution in the respective species.

In this paper, we use nucleotide sequences of protein-coding genes of mitogenomes to address the question if there were parallel changes in the rates of molecular evolution during adaptive radiation in the two species flocks of Baikalian amphipods.

2. Materials and methods

2.1. Mitochondrial genome sequences

Complete and nearly complete mitogenomes of amphipods available in GenBank by June 2019 were used in this paper: KX341962, KP161875 GU130250 AB539699 KX341963 MF361127 MF361126 KX341964 KF690638 KM287572 MF766257 JN704067 KY197961 MG779536 KX341965, KX341966 JN827386 LT594768 MH542433 LT594767 KX341967, FJ555185 KX341968 AY639937 MH542432 MG010370, MG010371 MH542430 MH229998, FR872382 - FR872383, HE860495 - HE860513, HE861923, FR872383, LN871175, LN871176, MH592123, MH592125 - MH592152, KU869711 - KU869713, MH542431,

*Corresponding author.

E-mail address: sherb@lin.irk.ru (D.Y. Sherbakov)

MK644228, MK354235, MK354236, and MH294484. Protein-coding genes were obtained according to the original annotations. The codon tables were also not verified, although the deduced amino acid sequences were checked for the absence of stop codons. All mitogenomes were downloaded separately and split into separate protein-coding genes that were translated and aligned using SeaView (Gouy et al., 2010) coupled with Mafft (Kato and Standley, 2013) and then operated with custom Biopython scripts (Cock et al., 2009) available from the authors.

2.2. Phylogenetic inferences

The Maximum Likelihood (ML) tree topology based on mitochondrial protein-coding genes of all amphipods were inferred from their combined amino acid sequences added by three crustacean species: *Eophreatocussp.14FK-2009* (FJ790313), *Ligia oceanica* (DQ442914), and *Neomysis japonica* (KR006340) as an outgroup, using IQ_TREE software (Nguyen et al., 2014). It was applied to the single partition containing

all combined amino acid sequences. The mtMet + F + R9 (nine categories of substitution rates) model was chosen using ModelFinder (Kalyaanamoorthy et al., 2017) built-in IQ_TREE. Both ST-*alrt* and ultra-fast bootstrap measures of statistical confidence were used. The tree obtained was further used as the topological constraint for the calculations of the base substitution rates within the separate protein-coding genes of the amphipods.

2.3. Rates of molecular evolution

Differences in rates of molecular evolution were estimated based on the nucleotide sequences of mitogenomes of the two independent lineages of Amphipods endemic to Lake Baikal, which are further assigned as “lineage1” and “lineage2”, and the genus *Gammarus* (Fig. 1). The latter provides two independent ancestors giving rise to the two Baikal species flocks (Hou and Sket, 2016).

A common ancestor of the Baikalian and *Gammarus* species was defined by the local outgroup *Onisimus nanseni*. The tree topology inferred from the

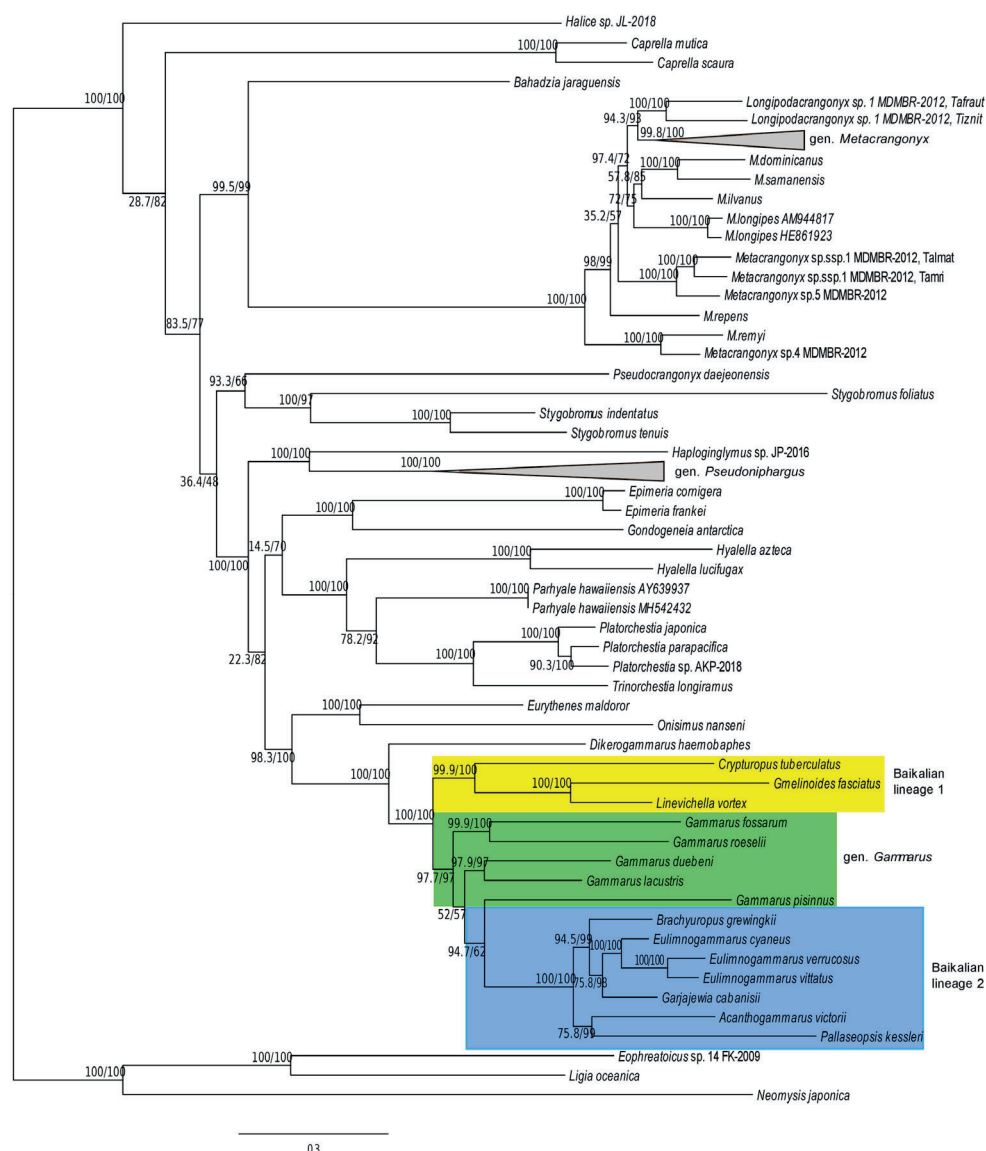


Fig. 1. ML phylogenetic tree of amphipods based on 13 amino acid sequences of mitochondrial protein-coding genes. Numbers at the branches correspond to ultrafast bootstrap support and relative rate test values (%). Clades of two Baikalian amphipod lineages and the representatives of gen. *Gammarus* group are highlighted in colors.

combined amino acid sequences of all mitochondrial protein-coding genes from available amphipod mitogenomes was used as the topological constraint for this study.

Nucleotide sequences of each protein-coding mitochondrial gene in all 94 mitogenomes studied were aligned separately, and the tree inferred from amino acid sequences was used as the topological constraint. IQ-TREE was applied to estimate branch lengths of this tree using a gene-specific model of molecular evolution. This model was determined for each gene using the ModelFinder (Kalyaanamoorthy et al., 2017). The summa of all tree edges connecting terminal leaves with the outgroup was taken to estimate the base substitution rate for each leaf.

Protein-coding genes CO1, CO2, CO3, Atp6, Atp8, Nad1, Nad5, and nad6 were used in the relative rate analysis. The other five standard mitochondrial genes were excluded from the analysis because of incomplete sequences in some crucial amphipod species. The significance of the difference in the substitution rates was tested with the Mann-Whitney non-parametric U-test (Mann and Whitney, 1947) between the groups of edge lengths for both Baikalian lineages and the *Gammarus* group.

3. Results and discussion

ML phylogenetic tree obtained in this study (Fig. 1), has highly supported topology similar to that previously described by Romanova et al. (2020). Minor difference dues to the few recently sequenced amphipod species included in the analysis: (*Dikerogammarus haemobaphes* (MK644228), *Halice* sp. JL-2018 (MH294484), *Gammarus lacustris* (MK354235), and *Gammarus pisinnus* (MK354236). Two latter species allowed us to obtain a better-supported separation between the Baikalian lineages.

For each mitogenome, the edge lengths between the leaf and the outgroup were calculated using ete2 Python library (Huerta-Cepas et al., 2010). The sequences were attributed to three groups as shown in Figure 1 by color boxes. The pairwise differences between the edge lengths of respective genes indicate that all genes evolve at obviously different rates (Fig. 2). There was also some acceleration between the two Baikalian lineages and the *Gammarus* lineage.

To estimate the significance of differences in the substitution rates between the groups of edge lengths for both Baikalian lineages and the *Gammarus* group, the accumulation of all pairwise differences between groups of sequences were calculated (Fig. 3). As the distributions of these differences were far from normal, the Mann - Whitney non-parametric U-test (Mann and Whitney, 1947) was used to find if the distribution median significantly differs from 0 or not (null hypothesis). The analysis showed no statistically significant differences in substitution rates in analyzed gene sequences of Baikalian amphipod lineages, except for the Cox1 and Nad6 genes. In these two cases, the acceleration in lineage 2 was significantly higher than in lineage 1.

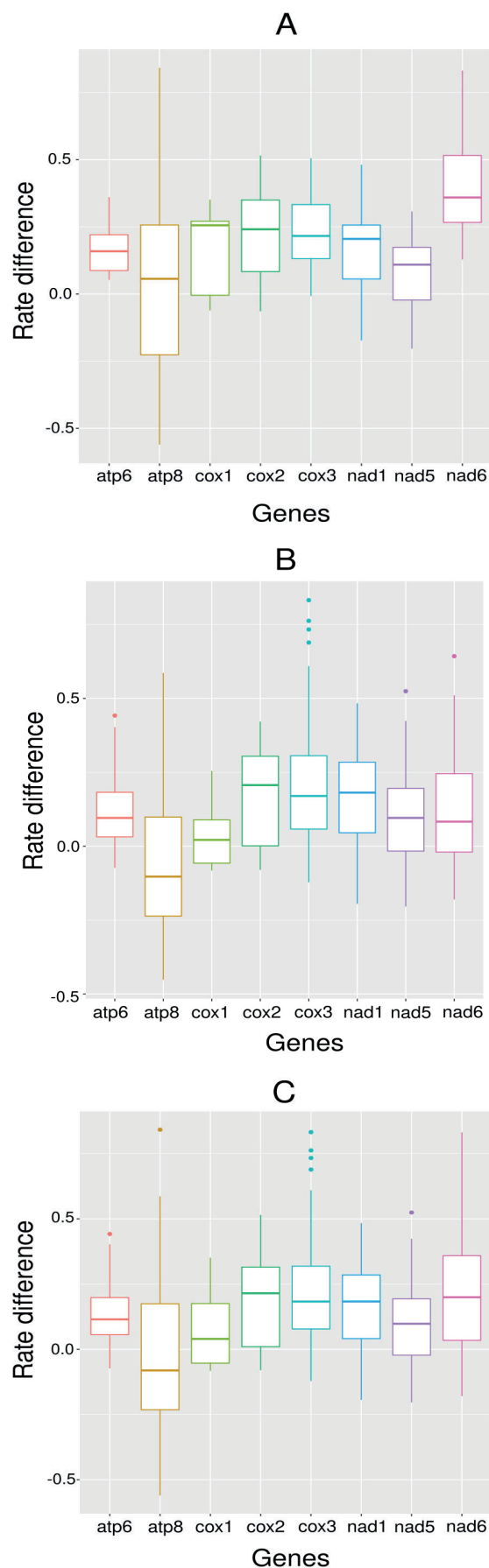


Fig. 2. Box plots of pairwise rate difference values. A – Difference between branch lengths of Baikalian amphipods from lineage 2 and the *Gammarus* group. B - Difference between branch lengths of Baikalian amphipods from lineage 1 and the *Gammarus* group. C – Difference between branch lengths of Baikalian amphipods from both Baikalian lineages and the *Gammarus* group.

The acceleration of substitution rates was detected, however, in both Baikalian lineages compared to the *Gammarus* group, except for Atp8 and Cox1 genes (Fig. 3, Table 1).

The results of the comparison indicate that the rate of molecular evolution in Baikalian amphipods is accelerated in almost all tested genes in parallel. The parallel acceleration of the molecular evolution rate may be explained by either a higher mutation rate in Lake Baikal or by some adaptive constraints specific to the lake. In the first case, one may expect that the difference accumulates faster in faster-evolving genes. In other words, a significant positive correlation between the average amount of difference in the average rates of the group and the rates of molecular evolution would suggest non-adaptive reasons for the acceleration in Lake Baikal. In Figure 4, the gene-specific acceleration in the rate is plotted against the average rates of molecular evolution in each gene. Since the differences were not normally distributed (Fig. 3),

Table 1. The result of testing the hypothesis about the acceleration of the molecular evolution rate in Baikalian amphipod lineages. Bold numbers indicate cases of statistically significant acceleration of substitution rate.

Gene	Pairwise differences between group members (p-values)		
	Lineage2-Lineage1	Lineage2-gen. <i>Gammarus</i>	Lineage1-gen. <i>Gammarus</i>
Atp6	0.1373	1.38E-07	6.00E-05
Atp8	0.1571	0.2383	0.7615
Cox1	0.0018	0.1954	6.70E-03
Cox2	0.055	2.16E-05	1.60E-03
Cox3	0.54	8.63E-08	1.20E-04
Nad1	1	1.07E-05	5.40E-03
Nad5	0.97	1.80E-03	0.04
Nad6	1.90E-06	2.70E-03	6.10E-05

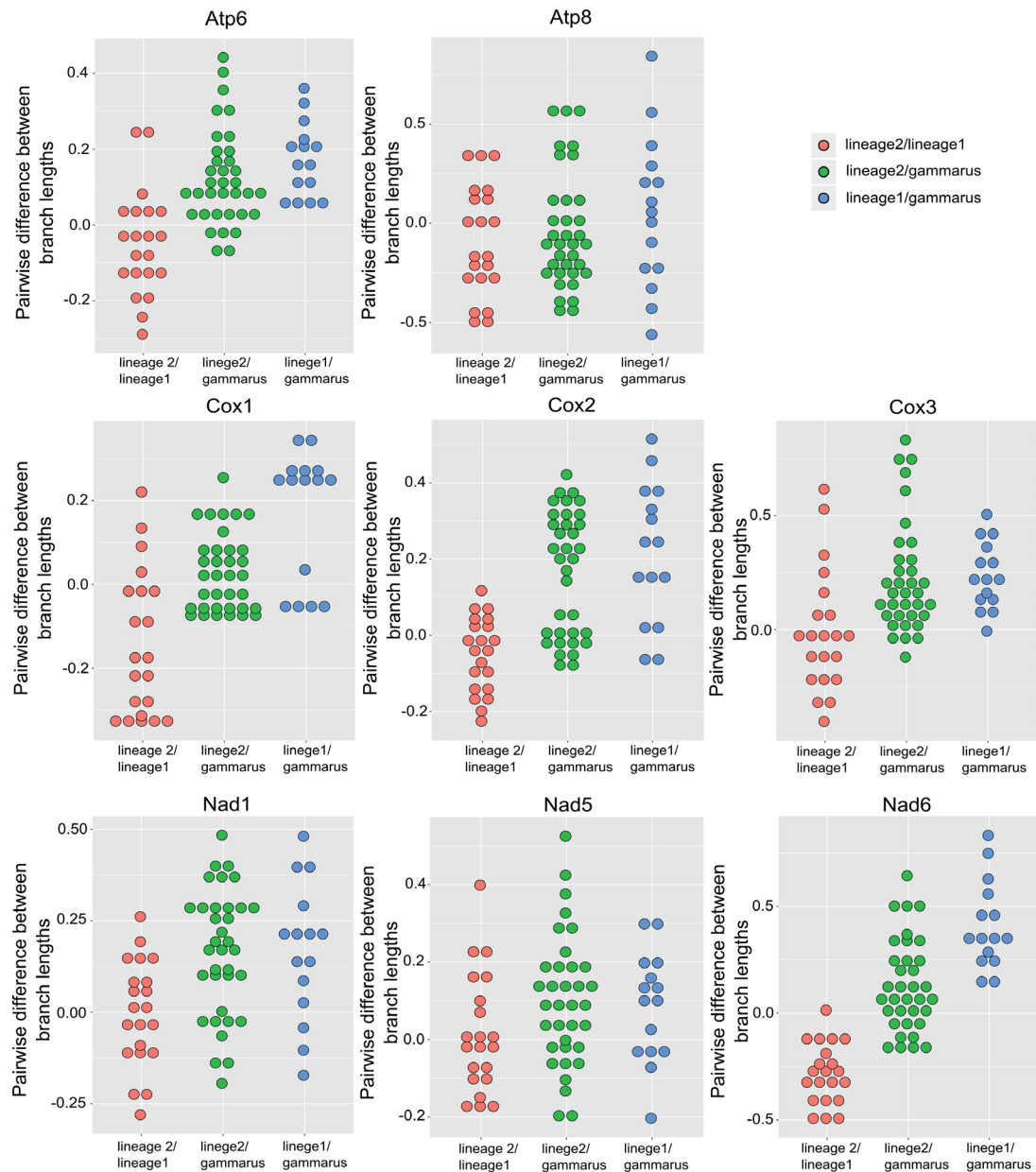


Fig. 3. Pairwise differences between branch lengths in different mitochondrial genes of amphipod groups of interest (Baikalian lineage 1, Baikalian lineage 2, gen. *Gammarus* group).

the Pearson rank correlation was estimated from the data to give a p -value of the hypothesis that it differs from 0 ($p > 0.6$). This favors the second hypothesis explaining the acceleration in molecular evolution by similar adaptive challenges in the parallel Baikalian amphipod lineages.

Our finding corroborates with the results by Naumenko et al. (2017), who detected episodes of positive selection in nuclear genes encoded components of electron transfer chain and ATP synthesis in Baikalian amphipods. It is also worth noticing that all currently available species of gen. *Gammarus* have the same conserved gene order in their mitogenomes, whereas the majority of Baikalian species in both lineages possess different types of gene rearrangements and additional tRNA gene copies (Romanova et al., 2016; 2020). Our analysis supports an opinion about the linkage of high evolutionary rate and gene rearrangements in mitogenomes (Shao et al., 2003; Fourdrilis et al., 2018).

Further studies of higher numbers of mitogenomes in combination with life history data and niche details of the respective species are required to elucidate the acceleration of molecular evolution in Baikalian endemic amphipods. Wider taxonomic sampling is required to test if the acceleration effect is general for Lake Baikal.

Acknowledgements

The study was supported by the governmentally funded project 0345–2019–0004 (AAAA - A16 - 116122110060 - 9).

References

- Bromham L., Cowman P.F., Lanfear R. 2013. Parasitic plants have increased rates of molecular evolution across all three genomes. *BMC Evolutionary Biology* 13. DOI: 10.1186/1471-2148-13-126
- Cock P.A., Antao T., Chang J.T. et al. 2009. Biopython: freely available Python tools for computational molecular biology and bioinformatics. *Bioinformatics* 25: 1422-1423. DOI: 10.1093/bioinformatics/btp163
- Cormier A., Wattier R., Teixeira M. et al. 2018. The complete mitochondrial genome of *Gammarus roeselii* (Crustacea, Amphipoda): insights into mitogenome plasticity and evolution. *Hydrobiologia* 825: 197-210. DOI: 10.1007/s10750-018-3578-z
- Ellegren H., Galtier N. 2016. Determinants of genetic diversity. *Nature Reviews Genetics* 17. DOI: 10.1038/nrg.2016.58
- Fazalova V., Nevado B., Peretolchina T. et al. 2010. When environmental changes do not cause geographic separation of fauna: differential responses of Baikalian invertebrates. *BMC Evolutionary Biology* 10: 988-999. DOI: 10.1016/j.ympev.2018.07.002
- Fourdrilis S., de Frias Martins A.M., Backeljau T. 2018. Relation between mitochondrial DNA hyperdiversity, mutation rate and mitochondrial genome evolution in *Melarhaphe neritoides* (Gastropoda: Littorinidae) and other Caenogastropoda. *Scientific Reports* 8: 1-12. DOI: 10.1038/s41598-018-36428-7
- Gouy M., Guindon S., Gascuel O. 2010. SeaView version 4: a multiplatform graphical user interface for sequence

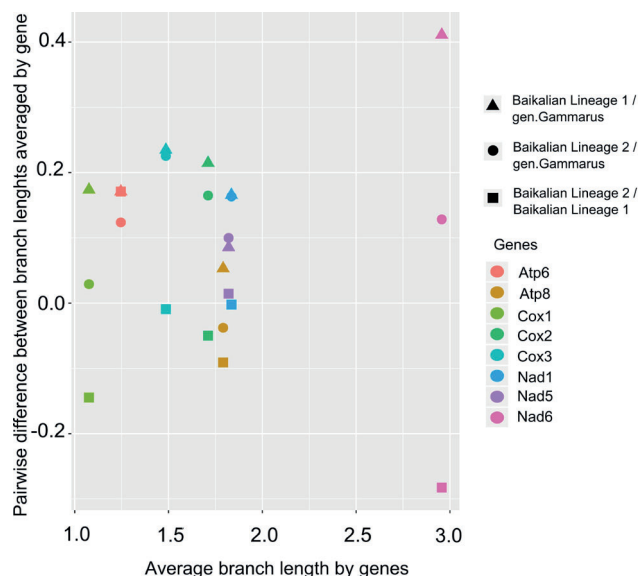


Fig. 4. The relation between the absolute branch length averaged by genes and the average pairwise difference in branch lengths averaged by genes and groups of sequences.

alignment and phylogenetic tree building. *Molecular Biology and Evolution* 27: 221-224. DOI: 10.1093/molbev/msp259

Hou Z., Sket B. 2016. A review of Gammaridae (Crustacea: Amphipoda): the family extent, its evolutionary history, and taxonomic redefinition of genera. *Zoological Journal of the Linnean Society* 176: 323-348. DOI: 10.1111/zoj.12318

Huerta-Cepas J., Dopazo J., Gabaldón T. 2010. ETE: a python Environment for Tree Exploration. *BMC Bioinformatics* 11. DOI: 10.1186/1471-2105-11-24

Kalyaanamoorthy S., Minh B.Q., Wong T.K. et al. 2017. ModelFinder: fast model selection for accurate phylogenetic estimates. *Nature Methods* 14. DOI: 10.1038/nmeth.4285

Kamaltynov R.M. 2009. Amphipoda: Gammaroidea in Angara and Yenisei rivers. In: Timoshkin O.A. (Ed.), *Index of animal species inhabiting Lake Baikal and its catchment area*. Novosibirsk, pp. 297-329. (in Russian)

Katoh K., Standley D.M. 2013. MAFFT multiple sequence alignment software version 7: improvements in performance and usability. *Molecular Biology and Evolution* 30: 772-780. DOI: 10.1093/molbev/mst010

Krebes L., Bastrop R. 2012. The mitogenome of *Gammarus duebeni* (Crustacea Amphipoda): a new gene order and non-neutral sequence evolution of tandem repeats in the control region. *Comparative Biochemistry and Physiology Part D: Genomics and Proteomics* 7: 201-211. DOI: 10.1016/j.cbd.2012.02.004

Lanfear R., Ho S.Y., Love D. et al. 2010. Mutation rate is linked to diversification in birds. *Proceedings of the National Academy of Sciences* 107: 20423-20428. DOI: 10.1073/pnas.1007888107

Macdonald III K.S., Yampolsky L., Duffy J.E. 2005. Molecular and morphological evolution of the amphipod radiation of Lake Baikal. *Molecular Phylogenetics and Evolution* 35: 323-343. DOI: 10.1016/j.ympev.2005.01.013

Macher J.N., Leese F., Weigand A.M. et al. 2017. The complete mitochondrial genome of a cryptic amphipod species from the *Gammarus fossarum* complex. *Mitochondrial DNA Part B* 2: 17-18. DOI: 10.1080/23802359.2016.1275844

Mann H.B., Whitney D.R. 1947. On a test of whether one of two random variables is stochastically larger than the other. *Annals of Mathematical Statistics* 18: 50-60.

Naumenko S.A., Logacheva M.D., Popova N.V. et al. 2017. Transcriptome-based phylogeny of endemic Lake Baikal amphipod species flock: fast speciation accompanied by frequent episodes of positive selection. *Molecular Ecology* 26: 536-553. DOI: 10.1111/mec.13927

Nguyen L.T., Schmidt H.A., von Haeseler A. et al. 2014. IQ-TREE: a fast and effective stochastic algorithm for estimating maximum-likelihood phylogenies. *Molecular Biology and Evolution* 32: 268-274. DOI: 10.1093/molbev/msu300

Pinkster S. 1983. The value of morphological characters in taxonomy of *Gammarus*. *Beaufortia* 33: 15-28.

Rabosky D.L. 2019. Phylogenies and diversification rates: variance cannot be ignored. *Systematic Biology* 68: 538-550. DOI: 10.1093/sysbio/syy079

Romanova E.V., Aleoshin V.V., Kamaltynov R.M. et al. 2016. Evolution of mitochondrial genomes in Baikalian amphipods. *BMC Genomics* 17. DOI: 10.1186/s12864-016-3357-z

Romanova E.V., Bukin Y.S., Mikhailov K.V. et al. 2020. Hidden cases of tRNA gene duplication and remodeling in mitochondrial genomes of amphipods. *Molecular Phylogenetics and Evolution* 144. DOI: 10.1016/j.ympev.2019.106710

Shao R., Dowton M., Murrell A. et al. 2003. Rates of gene rearrangement and nucleotide substitution are correlated in the mitochondrial genomes of insects. *Molecular Biology and Evolution* 20: 1612-1619. DOI: 10.1093/molbev/msg176

Sun S., Wu Y., Ge X. et al. 2020. Disentangling the interplay of positive and negative selection forces that shaped mitochondrial genomes of *Gammarus pisinnus* and *Gammarus lacustris*. *Royal Society Open Science* 7. DOI: 10.1098/rsos.190669

Wiens J.J., Scholl J.P. 2019. Diversification rates, clade ages, and macroevolutionary methods. *Proceedings of the National Academy of Sciences* 116: 24400-24400. DOI: 10.1073/pnas.1915908116

The role of atmospheric precipitation in the under-ice blooming of endemic dinoflagellate *Gymnodinium baicalense* var. *minor* Antipova in Lake Baikal

Obolkin V.A.¹, Volkova E.A.^{1*}, Ohira S.I.², Toda K.², Netsvetaeva O.G.¹,
Chebunina N.S.¹, Nosova V.V.¹, Bondarenko N.A.¹

¹ Limnological Institute, Siberian Branch of the Russian Academy of Sciences, Ulan-Batorskaya Str., 3, Irkutsk, 664033, Russia

² Department of Chemistry, Kumamoto University, 2-39-1 Kurokami, Kumamoto 860-8555, Japan

ABSTRACT. The mass development of the phototrophic under-ice community is an interesting phenomenon known for the Arctic Ocean as well as for some rivers and freshwater lakes, including Lake Baikal. Species composition and productive characteristics of the under-ice phytoplankton in Lake Baikal are well studied. During the under-ice blooming, an endemic dinoflagellate *Gymnodinium baicalense* var. *minor* Antipova can have more than half of the annual primary phytoplankton production. However, there are still many questions to be answered regarding the factors limiting abundance and proliferation of the under-ice phytoplankton as well as mechanisms facilitating it to persist in Lake Baikal under conditions of the low salinity and low temperature. In present work, we studied the development dynamics of dinoflagellates and microalgae under the ice cover in Listvennichny Bay of Lake Baikal from February to April 2018. Simultaneously, the dynamics of the chemical composition and concentration of atmospheric precipitation were analysed. We observed the under-ice community with the domination of endemic dinoflagellate *Gymnodinium baicalense* var. *minor* in April. The biomass of this species considerably varied on different days from 0.04 to 10.0 × 10³ mg/m³. The results of this study indicated that nutrient supply from precipitation could be an important source of nutrition for organisms developing under the ice, in particular, *Gymnodinium baicalense* var. *minor*, and could be one of the factors causing the fluctuations in its biomass. We suggested that abrupt significant increases in abundance of *G. baicalense* var. *minor* could be a result of their active migration to the area with elevated concentration of nitrogen from atmospheric precipitation. Such an ability may help this species to prosper under the ice of Lake Baikal.

Keywords: dinoflagellates, phytoplankton, the under-ice blooming, Lake Baikal, atmospheric precipitation

1. Introduction

In Lake Baikal, during the ice-cover period that lasts from February until May (Shimaraev et al., 1994), dinoflagellates and diatom microalgae play an important role as the main food source for protozoa and multicellular organisms (Kozhova, 1957; Antipova, 1963; Votintsev et al., 1975; Popovskaya, 2000). In the high-crop years of phytoplankton, the number of the dinoflagellates in the lake photic zone (0-50 m) under the ice cover can reach × 10⁶ cells/L making them the dominant species of the under-ice community (Kozhova, 1957; Antipova, 1963; Popovskaya, 2000). During spring in such years, endemic dinoflagellates of the genus *Gymnodinium* can have up to 65% of the annual primary phytoplankton production (Votintsev et al., 1975).

Dinoflagellates are a group of primarily unicellular organisms belonging to the Alveolata superphylum combined by a set of unique characteristics, such as flagellar insertion, pigmentation, organelles, and features of the nucleus that distinguish them from other groups (Belyakova et al., 2006; Carty and Parrow, 2015). They are widespread in aquatic systems, occupying various ecological niches, and show a high diversity and physiological variability, including phototrophy, heterotrophy, mixotrophy, and fish parasitism (Anderson, 1989; Carty, 2014). Under certain conditions, marine dinoflagellates can reproduce rapidly to form water blooms or red tides that colour water and may lead to fish kills (Landsberg, 2002; Hallegraeff, 2003). The bloom of some dinoflagellates in summer freshwater phytoplankton can be responsible for serious problems in drinking water quality (Carty

*Corresponding author.

E-mail address: cathvolkova@mail.ru (E.A. Volkova)

and Parrow, 2015). The dinoflagellate massive development can also occur under the ice cover both in marine (Spilling, 2007) and freshwater bodies (Phillips and Fawley, 2002; Carty and Parrow, 2015), including Lake Baikal (Votintsev et al., 1975; Obolkina et al., 2000; Annenkova et al., 2009; Bondarenko et al., 2012; Bashenkhaeva et al., 2015; 2017).

There are numerous studies on the species composition, abundance, duration of vegetation, and productive characteristics of the under-ice phytoplankton in Lake Baikal (e.g. Antipova and Kozhov, 1953; Kozhova, 1961; Antipova, 1963; Votintsev et al., 1975; Obolkina et al., 2000; Popovskaya, 2000; Bondarenko et al., 1996; 2012; 2013; Bashenkhaeva et al., 2015; 2017). However, there are still many questions to be answered regarding the factors limiting abundance and proliferation of the phytoplankton as well as mechanisms facilitating it to persist in Lake Baikal under the ice cover at the low salinity and low temperature. In the present work, we studied seasonal dynamics of the *Gymnodinium baicalense* var. *minor* abundance during its blooming under the ice cover in Listvennichny Bay of Lake Baikal in 2018, and discuss possible effects on this dynamics of some abiotic factors, such as nutrients intake from atmospheric precipitation.

2. Methods

Species composition, total abundance, and biomass of dinoflagellates and microalgae from under the ice were studied using samples from the surface water of ice holes collected at a depth of 600 m in Listvennichny Bay of Lake Baikal from February to April 2018. Geographical coordinates of the sampling site are 51°51'49"N, 104°50'093"E. Samples were fixed with the Utermohl's solution in 0.5-1.0 L plastic bottles and concentrated by sedimentation for 10 days (Kiselev, 1956). The species composition and cell number were estimated in triplicate for each sample using the Fuchs-Rosenthal counting chamber with a grid of 3.2 µl and an area of 16 mm², and an Olympus CX 21 light microscope (Tokyo, Japan) at ×20, and ×40 magnification. The species were identified using monographs "Diatomovye vodorosli..." (1988; 1992) and the keys by Matvienko and Litvinenko (1977), Popovskaya et al. (2011). The biomass was estimated by the cell true volume method according to Belykh et al. (2011). The cell volume of each species was determined according to their average size measured under the microscope. The average cell volume of *Gymnodinium baicalense* var. *minor* was calculated by the formula according to Belykh et al. (2011) given for *Gymnodinium baicalense* Antipova and was 23900 µm³. The growth rate of *Gymnodinium baicalense* var. *minor* was calculated by the formula $\mu = (\ln N_1 - \ln N_0) / t$, where N_0 and N_1 are the numbers of cells at time moments t_0 and t_1 , and t is the time difference between the samples.

The chemical composition and concentration of atmospheric precipitation (each case) were analysed from January to April 2018. The chemical analysis was carried out according to conventional freshwater chemistry methods (Rukovodstvo..., 2009; Khodzher et

al., 2017; Wetzel and Likens, 1991) at the accredited Laboratory of the Hydrochemistry and Atmosphere Chemistry of Limnological Institute SB RAS using the equipment of the collective instrumental centre 'Ultramicroanalysis'. The nutrient content in the filtered water was measured using the following colorimetric methods: indophenol blue method for NH_4^+ , Griss's method for NO_2^- , Deniges's method for PO_4^{3-} , and the ammonium molybdate method for Si (Khodzher et al., 2017). Nitrate NO_3^- in the filtrates was quantified using ionic chromatography on an ICS-3000 ionic system (Dionex, USA).

Data on the air temperature dynamics in the fieldwork area were provided by the local weather station 'Istok Angara'.

3. Results

In 2018, the ice cover in Listvennichny Bay of Lake Baikal formed on 23 January; it lasted until 27 April and was fully broken on 7 May. The maximum ice thickness in the fieldwork area was ca. 80 cm at the end of March. The water temperature under the ice was approximately 0 °C. The air temperature varied from −25.0 to +20.0 °C between February and April, starting to gradually increase in the early March and reaching positive values by the end of this month (Fig.1).

The nutrient concentrations measured in snow and rain precipitation varied considerably (Table 1). There was a significant difference between the average concentration of the ions in atmospheric precipitation and the lake water (Fig. 2, Table 1). Specifically, the

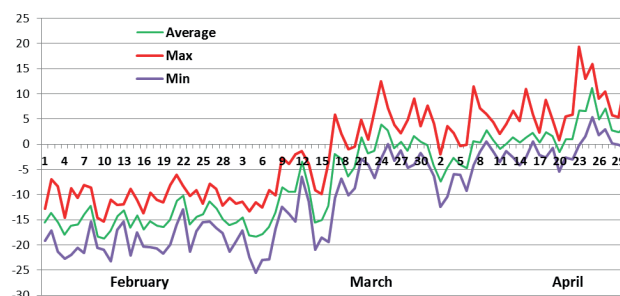


Fig.1. Daily fluctuations in the air temperature in Listvennichny Bay, Lake Baikal, 2018

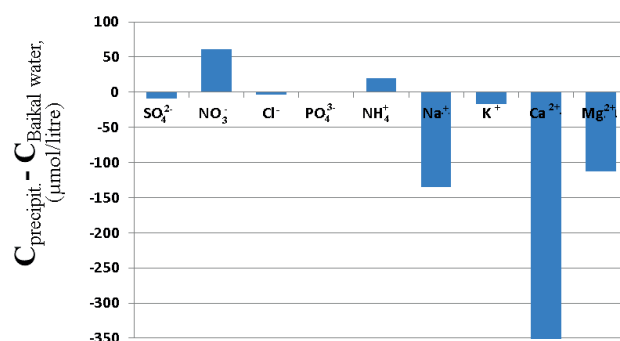


Fig.2. The difference of average ion concentrations in precipitation from February to May 2018 and in the Lake Baikal water according to Grachev (2002)

Table 1. Chemical composition of atmospheric precipitation during January-April 2018 and of the Lake Baikal water (Grachev, 2002).

Precipitation period		Precip.-amount, mm	Concentration, $\mu\text{mol/l}$										Deposition, $\mu\text{mol/m}^2$		
			SO_4^{2-}	NO_3^-	Cl^-	PO_4^{3-}	NH_4^+	Na^+	K^+	Ca^{2+}	Mg^{2+}	H^+	NO_3^-	NH_4^+	PO_4^{3-}
12.01.18	13.01.18	2.4	30.0	74.3	4.8	0.3	11.7	5.7	3.1	43.2	8.6	7.9	178.3	28.1	0.6
19.01.18	20.01.18	0.9	67.6	80.4	11.6	0.1	5.7	6.5	7.4	128.5	25.5	0.2	72.4	5.1	0.1
27.01.18	28.01.18	1.2	58.3	71.3	11.9	0.0	2.6	10.0	2.8	96.8	16.0	1.0	85.6	3.1	0.0
07.02.18	08.02.18	2.1	43.2	76.4	9.3	0.0	8.9	5.7	2.3	61.4	10.7	4.9	160.4	18.7	0.0
08.02.18	09.02.18	2.7	20.3	44.9	8.2	0.1	6.7	7.8	3.1	29.9	5.3	5.2	121.2	18.0	0.2
12.02.18	13.02.18	2.8	19.4	37.4	9.7	0.0	2.6	5.2	3.1	30.4	5.8	3.8	104.7	7.3	0.1
20.02.18	21.02.18	1.2	53.4	91.5	13.8	0.1	4.8	9.6	5.6	71.3	16.4	4.0	109.8	5.8	0.1
25.02.18	26.02.18	4.2	21.2	47.1	2.9	0.0	11.1	3.5	1.5	25.7	5.3	11.2	197.8	46.6	0.2
03.03.18	04.03.18	3.1	22.1	44.9	6.5	0.1	12.2	6.5	3.1	26.9	4.9	8.5	139.2	37.8	0.2
11.03.18	12.03.18	2.4	42.7	73.2	6.3	0.1	25.5	7.8	3.8	45.7	9.0	12.3	175.7	61.2	0.2
24.03.18	25.03.18	1.4	45.3	55.0	5.0	0.2	37.2	7.0	5.6	38.4	8.6	4.4	77.0	52.1	0.3
08.04.18	09.04.18	1.9	145.7	206.8	17.6	0.6	98.3	27.0	21.5	136.5	31.2	17.0	392.9	186.8	1.1
18.04.18	19.04.18	2.7	14.6	9.1	5.4	0.3	17.0	4.8	1.3	10.7	1.6	4.9	24.5	45.9	0.8
26.04.18	27.04.18	2.6	38.1	36.8	3.4	1.4	51.2	3.9	18.2	22.5	6.2	7.4	95.7	133.1	3.7
Average in precipitation		Sum 31.6	44.4	67.8	8.3	0.2	21.1	7.9	5.9	54.9	11.1	6.6	Total deposition		
													1935	650	7.6
Baikal water (average)			54	6.4	11	0.21	~ 1	143	23	407	123	0.02			
Ratio $C_{\text{precip.}}/C_{\text{lake water}}$			0.82	10.6	0.75	0.95	21.1	0.06	0.26	0.13	0.09	330			

concentration of phosphate (PO_4^{3-}) was nearly the same in precipitation as in the lake water (Table 1); however, the concentrations of nitrate (NO_3^-) and ammonium (NH_4^+) were 10-20 times higher in precipitation (Table 1).

In 2018, the dinoflagellate *Gymnodinium baicalense* var. *minor* and some microalgae represented the under-ice community in Lake Baikal. Cryptomonads *Rhodomonas pusilla* (Bachmann) Javornicky and *Cryptomonas* spp. Ehrenberg, as well as green alga *Koliella longiseta* (Vischer) Hindak, prevailed in the community from February until April. During this period, there was a gradual increase in the number of these species and the diatom *Fragilaria radians* (Kützinger) Williams & Round in the 0-m water layer under the ice cover (Fig. 3, Fig. 4). The following microalgae were the minor or irregular components of the under-ice community at this depth: *Nitzschia graciliformis* Lange-Bertalot & Simonsen emend Genkal et Popovskaya, *Lindavia minuta* (Skvortzow) Nakov et al., *Monoraphidium* sp. Komarkova-Legnerova, *Dinobryon cylindricum* Imhof, *Chrysococcus* sp. Klebs, *Synechococcus* sp. Nägeli.

From the late February until March, single specimens of dinoflagellates were observed. A significant increase in *G. baicalense* var. *minor* was in early April (Fig. 3, Fig. 4). The biomass of *G. baicalense* var. *minor* in the lake water from the ice-hole generally tended to increase but varied on different days from 0.04 to 10.0 $\times 10^3$ mg/m³.

During the entire study period, other

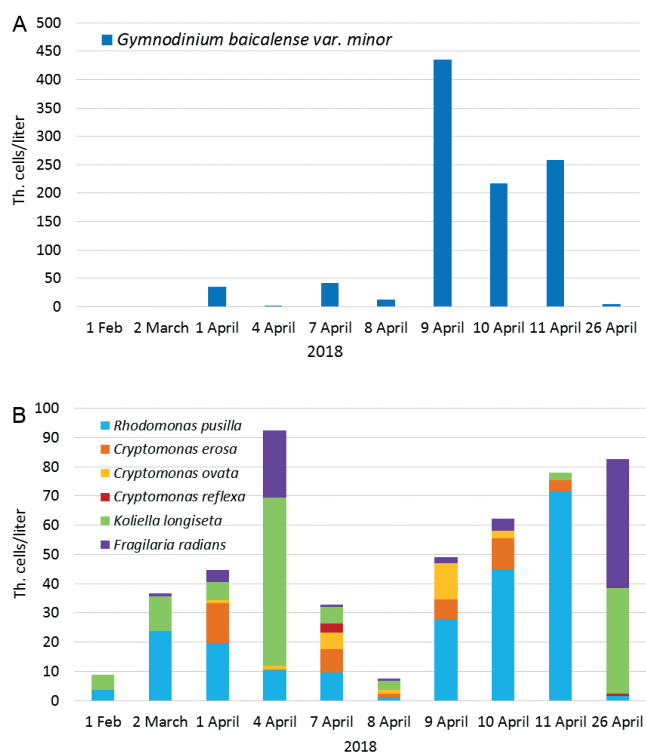


Fig.3. Seasonal changes in abundance of *Gymnodinium baicalense* var. *minor* (A) and dominant microalgae (B) in the 0-m water layer, Listvennichny Bay, Lake Baikal, 2018

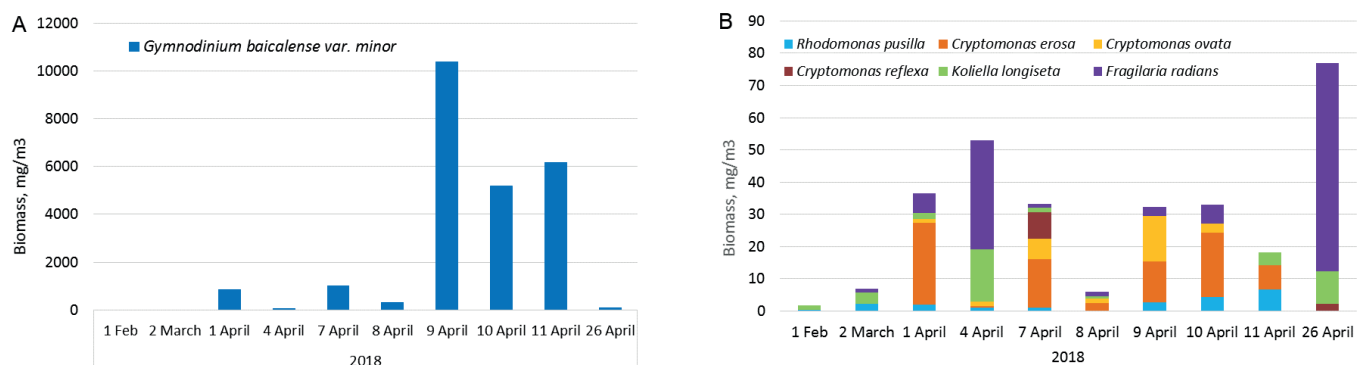


Fig.4. Seasonal changes in biomass of *Gymnodinium baicalense* var. *minor* (A) and dominant microalgae (B) in the 0-m water layer of Listvennichny Bay, Lake Baikal, 2018

dinoflagellates known for Lake Baikal, such as *Gymnodinium baicalense* Antipova, *Gyrodinium helveticum* (Penard) Takano & Horiguchi, *Apocalathium baicalense* (Kiselev & Zvetkov) Craveiro, Daugbjerg, Moestrup & Calado, *Apocalathium* sp., were present as single cells or cysts.

A sharp increase in *G. baicalense* var. *minor* after the night precipitation with high nutrient concentration was observed on 9 April (Fig. 3, Fig. 4; Table 1). The massive development of *G. baicalense* var. *minor* manifested in the form of dense yellow masses having several centimetres in diameter on the walls of the ice-holes and cracks as well as in the lower layer of the ice cover (Fig. 5, Fig. 6). A decline in the development of *G. baicalense* var. *minor* was at the end of April (Fig. 3, Fig. 4).

4. Discussion

Development of Gymnodinium baicalense var. *minor* under the ice cover in 2018

In 2018, we observed the under-ice community with the domination of endemic dinoflagellate *Gymnodinium baicalense* var. *minor* in Listvennichny Bay of Lake Baikal. The development pattern of this species was quite typical according to other reports (Antipova, 1955; Kozhova, 1959; Votintsev et al., 1975; Obolkina

et al., 2000; Bondarenko et al., 2012). Specifically, the abundance of its cells in the surface water of the lake was low in February but significantly raised in April. In previous years, the development of this species was characterized by substantial outbreaks of its biomass with the subsequent decline (Antipova, 1955; Kozhova, 1959; Votintsev et al., 1975; Annenkova et al., 2009). In 2018, there were also significant and sharp increases in abundance of *G. baicalense* var. *minor* that caused temporary yellow colouring of the lake water and the ice cover. The biomass of *G. baicalense* var. *minor* in the lake water was irregular and considerably varied on different days. However, this variability was in a range documented for this species in other studies (Kozhova, 1960; Votintsev et al., 1975). For example, Votintsev et al. (1975) reported that the biomass of *G. baicalense* var. *minor* ranged between 0.65 and 40.0 g/m³ in the surface waters of the lake. The biomass of the microalgae in 2018 also varied, but it was significantly lower than the biomass of *G. baicalense* var. *minor*.

Atmospheric recipitation as an important source of nutrients for the development of the under-ice community in Lake Baikal

The phenomenon of the mass development of the phototrophic under-ice community in Lake Baikal has received a great attention in scientific literature (e.g.

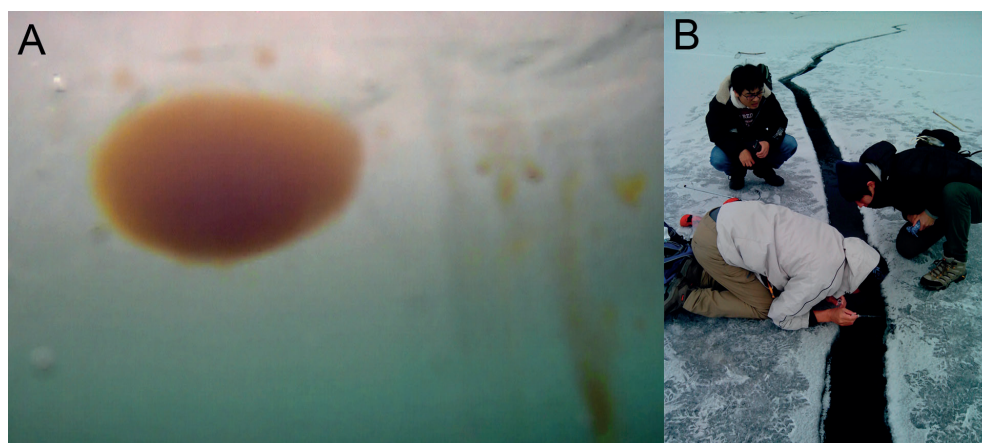


Fig.5. The concentration of *Gymnodinium baicalense* var. *minor* on the walls of the ice hole in the Lake Baikal ice cover, and its mass release to the water column from the ice interstitial (A); an ice crack where the concentration of dinoflagellates was typically observed (B)

Kozhov, 1955; Kozhova, 1961; Obolkina et al., 2000; Jewson et al., 2009; Evstafiev et al., 2010; Bondarenko et al., 2013, etc.). It is rather peculiar and occurs due to exceptional purity and transparency of the Baikal ice, as ca. 65-80 % of solar radiation penetrates through it enabling microalgae and dinoflagellates to develop (Shimaraev et al., 1994; Jewson et al., 2009). Since the transparency of the ice greatly reduces when it becomes covered with snow, it was considered that the under-ice extensive development of phytoplankton, which usually starts in February, most likely depended on releasing of the lake ice cover from snow by winds that normally were especially strong in that month (Kozhov, 1955; Kozhova, 1961). However, no strong relations between the under-ice phytoplankton and the thickness of the snow cover, as well as the wind activity, have been determined (Kozhova, 1961; Bashenkhaeva et al., 2015). Although the example of the under-ice community in marine ecosystems (Róžańska et al., 2009) and recently in Lake Baikal showed that diatom microalgae tended to develop under the ice partially covered with snow (Jewson et al., 2009; Bashenkhaeva et al., 2015), whereas dinoflagellates dominated the under-ice community under the maximum snow cover (Bashenkhaeva et al., 2015). Therefore, even though an increase in solar radiation availability can affect the beginning of the under-ice development of the species capable of phototrophy, it is unlikely the key factor determining their enormous abundance and biomass. No direct relation was found between nutrients and the under-ice phytoplankton in the lake (Votintsev, 1975; Kozhova, 1961). Nonetheless, in addition to the solar radiation, a suitable environment within and under the ice as well as the availability of nutrients should be crucial for microalgae and dinoflagellates to persist and develop in such extreme conditions. For example, Obolkina et al. (2000) revealed that development of cryophilic community in Lake Baikal was associated with occurrence of the numerous capillaries in the ice filled with water, whilst only cysts and resting stages were detected in the solid phase of newly formed ice cover (Obolkina et al., 2000; Bondarenko et al., 2012; 2013).

During the ice-cover period, which lasts for four-five months on Lake Baikal (Shimaraev et al., 1994), there is a limited influx of nutrients due to the absence of the wind-wave mixing of water masses (Kozhova, 1961). The results of our study suggest that nutrient supply from precipitation can be an important source of nutrition for organisms developing under the ice in Lake Baikal. In particular, in 2018, the concentrations of nitrates and ammonium were 10 and 20 times higher, respectively, than their average concentrations in the Lake Baikal water. (Fig. 2, Table 1). A significant rise in the air temperature to +5 +10° C in the late March (Fig. 1) caused melting of the upper layer of the ice, resulting in the seepage of the melt-water with nutrients accumulated from precipitation into capillaries of the ice cover. Usually, the development of the under-ice phytoplankton in Lake Baikal is maximum during March and April (Kozhova, 1960; Votintsev et al., 1975; Obolkina et al., 2000). Evidently, acquiring a structure permeated with capillaries and pores by the ice and its further saturation with water facilitates the effective penetration of nutrients from the melt precipitation, making them available for phytoplankton. Mineralisation of the organisms that massively developed in the capillaries of the ice was shown to provide an intake of nitrates and ammonium (Bondarenko et al., 2013). However, we propose that initial increase in abundance and biomass of the under-ice phototrophic community in Lake Baikal, like in April 2018, is likely enhanced by nutrients from atmospheric precipitation.

Atmospheric precipitation is an important source of nutrients for freshwater ecosystems (Russell et al., 1998; Zhai et al., 2009; Chen et al., 2018), especially when the water masses are limited by poor mobility and mixing; thus, they are sensitive to atmospheric nutrient inputs (Zheng et al., 2019). The fluctuations in abundance of microalgae and dinoflagellates in Lake Baikal, which were especially significant in April 2018 (Fig. 3, Fig 4), could be due to fluctuations in the nutrient concentration released with precipitation into the lake water and the flooded ice. A further short-term decrease in the air temperature at the beginning

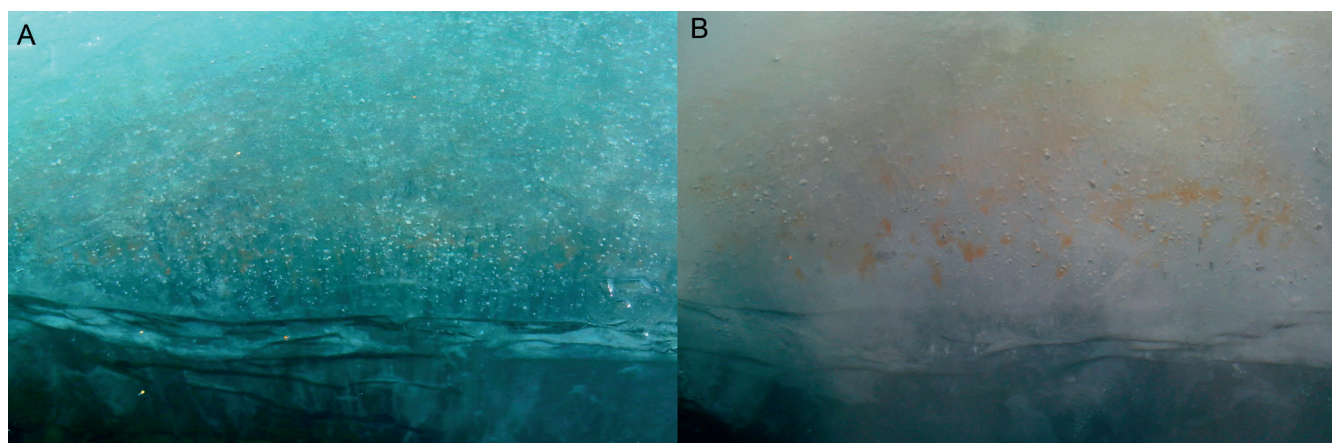


Fig.6. The flooded ice floe on 8 April before the rain precipitation (A) and the same ice floe after the rain precipitation at night on 9 April with concentration of dinoflagellates, mostly *Gymnodinium baicalense* var. *minor* (yellow spots), in the water above the ice (B)

of April stopped the ice melting and, consequently, the influx of nutrients. This might result in a decline of some microalgae and dinoflagellates in the lake water. Accordingly, the further sharp increase in the number of *G. baicalense* var. *minor* on 9 April (Fig. 3 - Fig. 6) could be related to the rain precipitation at night on 9 April that had exceptionally high nutrient concentrations, in particular, nitrogen (Table 1). Dinoflagellates are capable of assimilating nitrogen both in the form of nitrates and ammonium (Dagenais-Bellefeuille and Morse, 2013). They also can temporarily accumulate inorganic and organic nitrogen available in the environment (Maguer et al., 2007; Kopp et al., 2013).

High concentrations of certain nutrients can be toxic for dinoflagellates (Chang and McClean, 1997). For instance, NH_4^+ concentrations higher than 25 $\mu\text{mol/l}$ inhibit the growth of *Alexandrium minutum* Halim (Chang and McClean, 1997). However, in Lake Baikal, high concentrations of nutrients from precipitation could be substantially diluted with the lake water, which has an extraordinary low salinity (Grachev, 2002). Thus, the rain precipitation at night on 9 April was relatively small, ca. 1.9 mm (Table 1), but it had a high NH_4^+ concentration of 98 $\mu\text{mol/l}$ (Table 1), whereas the water layer above the flooded ice cover, where we observed the massive yellow accumulations of *G. baicalense* var. *minor* (Fig. 5, Fig. 6), was ca. 100 mm. The total concentration of the NH_4^+ after mixing of precipitation with the lake water should be deluded up to 50 times (100 mm/2 mm). Therefore, the concentration of NH_4^+ increased but not significantly, and, instead of average 1 $\mu\text{mol/l}$ (Grachev, 2002), it could reach 3 $\mu\text{mol/l}$ in the lake water, which should favour the development of dinoflagellates and microalgae but not inhibit it. During the next few days after the rain precipitation, the abundance of *G. baicalense* var. *minor* and microalgae decreased (Fig. 3, Fig. 4, Fig. 6). This might be because of a decrease in the concentration of nutrients due to its dilution with the lake water and/or its active assimilation by dinoflagellates and algobacterial community (Bondarenko et al., 2013; Bashenkhaeva et al., 2017). For example, previous studies revealed that the lowest concentration of ammonium and nitrates were in the areas with the highest abundance of the organisms in the ice cover, which indicated active assimilation processes (Bondarenko et al., 2013). Grazing may be another factor affecting the abundance of microalgae and dinoflagellates under the ice, and it requires special research.

Although no relevant studies have been carried out for *G. baicalense* var. *minor*, specifically, many dinoflagellates considered as phototrophic are capable of mixotrophic nutrition (Kirchner et al., 1996). Particularly, some dinoflagellates feed on nitrogen-fixing cyanobacteria *Synechococcus* spp. (Jeong et al., 2005). Therefore, the accelerated development of *G. baicalense* var. *minor*, in addition to its direct assimilation of NO_3^- and NH_4^+ , could be due to its ability to consume bacteria. The total amount of bacteria in the under-ice microbial community of Lake Baikal can be several times higher than in the melt-water of the

ice cover as well as in the photic zone (0-25-50 m) of the lake (Bondarenko et al., 2013; Bashenkhaeva et al., 2017). A potential mixotrophy could help *G. baicalense* var. *minor* to develop under the ice cover with a thick snow layer (Bondarenko, 1995; Bashenkhaeva et al., 2015; 2017).

The role of migrations for Gymnodinium baicalense var. *minor*

The abrupt changes in the abundance of *G. baicalense* var. *minor* in the surface water layer, in particular, its increase, were quite remarkable. For example, it increased from 13×10^3 to 430×10^3 cells/litre after the night on 9 April. If such an increase in abundance was only due to cell division, the generation rate of the species should be equal to 3.5 cell divisions per day. However, according to the estimation in Votintsev et al. (1975), the generation rate of this dinoflagellate in the lake does not exceed a range of 0.2 – 1.2 divisions per day. In this regard, a more likely cause of such an abrupt increase in the abundance of this species may be its ability to actively migrate. Some marine dinoflagellates are capable of migration to the ocean areas with limited light availability but having the concentration of nitrates higher than on the water surface where the species are normally concentrated (Harrison, 1976; Smayda, 1997). These migrations were rather associated with reaction to nutrients availability than with circadian rhythms depending on the availability of solar radiation (Harrison, 1976; Smayda, 1997). The fact that variations in NO_3^- concentrations affect the endogenous clock of *Lingulodinium polyedra* (Stein) Dodge, regulating its migrations, also supports this hypothesis (Roenneberg and Rehman, 1996). Furthermore, dinoflagellates are among the fastest phytoflagellate swimmers: the swimming speed of many species is 0.2 – 2 meters per hour, and for some species, it reaches up to 5 m per hour (Kamykowski, 1995). Our observations in 2018 may also indicate the active migration of *G. baicalense* var. *minor* towards the higher nutrient concentration (Fig. 6). This can be one of the reasons for the fluctuations of its abundance in the surface water. Potential capacity for such rapid movement along with effective nitrogen accumulation may help *G. baicalense* var. *minor* to compete with other protists and occupy its ecological niche in the under-ice conditions of Lake Baikal.

5. Conclusion

The under-ice bloom of phytoplankton is highly important for the ecosystem of Lake Baikal, as it can have most of the annual primary production. The present study showed that atmospheric precipitation could be an important source of nutrition for the under-ice organisms in Lake Baikal where the water masses are limited by mobility, which prevents the influx of nutrients from the underlying water layers. An appropriate structure of the loose ice cover permeated with pores and capillaries apparently facilitates the effective penetration of nutrients from

the melted precipitation, making them available for phytoplankton. The chemical analysis revealed that atmospheric precipitation in 2018 had nearly the same concentration of phosphate as the Lake Baikal water on average but elevated concentrations of nitrate and ammonium. We suggested that nutrients from precipitation, in particular, nitrogen, could be one of the key factors enhancing the mass development of the under-ice community in Lake Baikal. The endemic dinoflagellate *G. baicalense* var. *minor* dominated microalgae in the surface waters and the ice cover in April 2018, but its abundance varied significantly on different days. We proposed that such development dynamics of *G. baicalense* var. *minor* could be partly owing to its capacity for an active migration towards the high nitrogen concentration initially released into water from atmospheric precipitation. Atmospheric precipitation as a source of nutrients should not be underestimated as a driving force for the under-ice community and its potential influence on primary production, especially during the ongoing ecological changes in Lake Baikal.

Acknowledgments

The study was supported by Bilateral Program Joint Research Project No.18-55-50001 YaF_a from the Russian Foundation for Basic Research (RFBR) and Japan Society for the Promotion of Science (JSPS) 'Investigation of biogenic chemicals produced by Lake Baikal phytoplankton during its under-ice blooming'. Authors thank Dr. N.V. Annenkova for her critical comments and valuable suggestions on the paper and significant contribution to the discussion on the active migration of dinoflagellates.

References

- Annenkova N.V., Belykh O.I., Denikina N.N. et al. 2009. Identification of dinoflagellates from Lake Baikal on the basis of molecular genetic data. *Doklady Biological Sciences* 426: 253-256. DOI: 10.1134/S001249660903@@@
- Antipova N.L., Kozhov M.M. 1953. Materials on seasonal and annual fluctuations in the number of leading forms of phytoplankton of Lake Baikal. *Trudy Irkutskogo Gosudarstvennogo Universiteta. Seriya "Biologiya"* [Proceedings of the Irkutsk State University. Series "Biology"] 7: 63-68. (In Russian)
- Antipova N.L. 1955. New species of the genus *Gymnodinium* Stein (Gymnodiniaceae) in Lake Baikal. *Doklady Akademii Nauk USSR* [Proceeding of the USSR Academy of Sciences] 103: 325-328. (in Russian)
- Antipova N.L. 1963. On fluctuations in the number of species of Melozira in the plankton of Lake Baikal. *Trudy Vsesoiuznogo Gidrobiologicheskogo Obshchestva* [Proceedings of the All-Russian Hydrobiological Society] 8: 235-241. (in Russian)
- Anderson D.M. 1989. Toxic algal blooms and red tides: a global perspective. In: Okaichi T., Anderson D.M., Nemoto T. (Eds.), *Red tides: Biology, environmental science and toxicology*. New York, pp. 11-16.
- Bashenkhaeva M.V., Zakharova Y.R., Petrova D.P. et al. 2015. Sub-ice microalgal and bacterial communities in freshwater Lake Baikal, Russia. *Microbial Ecology* 70: 751-765. DOI: 10.1007/s00248-015-0619-2
- Bashenkhaeva M.V., Zakharova Yu.R., Galachyants Yu.P. 2017. Bacterial communities during the period of massive under-ice Dinoflagellate development in Lake Baikal. *Microbiology* 86: 524-532. DOI: 10.1134/S0026261717040038.
- Belyakova G.A., D'yakov Yu.T., Tarasova K.L. 2006. *Botanika. Vol. 1: Vodorosli i griby*. Moscow: Akademia. (in Russian)
- Belykh O.I., Bessudova A.Y., Gladkikh A.S. et al. 2011. *Rukovodstvo po opredeleniyu biomassy vidov planktona pelagiali oz. Baikal*. Irkutsk: Irkutsk State University. (in Russian)
- Rukovodstvo pokhimicheskomu analizu poverkhnostnykh vod sushi. Part 1. 2009. In: Boeva L.V. (Ed.). *Rostov-on-Don: NOK*. (in Russian)
- Bondarenko N.A. 1995. *Svobodnozhivushchie zhgutikovye. Ecologia*. In: Timoshkin O.A. (Ed.), *Atlas i opredelitel' pelagobiontov Baikala*. Novosibirsk, pp. 179-181. (in Russian)
- Bondarenko N.A., Guselnikova N.E., Logacheva N.F. et al. 1996. Spatial distribution of phytoplankton in Lake Baikal, spring 1991. *Freshwater Biology* 35: 517-523. DOI: 10.1111/j.1365-2427.1996.tb01765.x
- Bondarenko N.A., Belykh O.I., Golobokova L.P. et al. 2012. Stratified distribution of nutrients and extremophile biota within freshwater ice covering the surface of Lake Baikal. *The Journal of Microbiology* 50: 8-16. DOI: 10.1007/s12275-012-1251-1
- Bondarenko N.A., Belykh O.I., Golobokova L.P. et al. 2013. Chemical composition, bacterial and algae communities of Lake Baikal ice. *Hydrobiological Journal* 1: 14-28. DOI: 10.1615/HydrobJ.v49.i3.20.
- Carty S. 2014. *Freshwater Dinoflagellates of North America*. Ithaca, NY: Cornell University Press.
- Carty S., Parrow M.W. 2015. Dinoflagellates. In: Wehr J., Sheath R., Kociolek J.P. (Eds.), *Freshwater algae of North America: Ecology and classification*. San Diego, CA, pp. 773-807.
- Chang F.H., McClean M. 1997. Growth responses of *Alexandrium minutum* (Dinophyceae) as a function of three different nitrogen sources and irradiance. *New Zealand Journal of Marine and Freshwater Research* 31: 1-7. DOI: 10.1080/00288330.1997.9516740
- Chen X., Wang Y-H., Chun Y. et al. 2018. Atmospheric nitrogen deposition associated with the eutrophication of Taihu Lake. *Hindawi Journal of Chemistry* 2018. DOI: 10.1155/2018/4017107.
- Dagenais-Bellefeuille S., Morse D. 2013. Putting the N in dinoflagellates. *Frontiers in Microbiology* 4. DOI: 10.3389/fmicb.2013.00369.
- Evstafiev V.K., Bondarenko N.A., Mel'nik N.G. 2010. Long-term analysis of main trophic links dynamics in the Lake Baikal pelagic zone. *Izvestiya Irkutskogo Gosudarstvennogo Universiteta. Seriya "Biologiya. Ekologiya"* [The bulletin of Irkutsk State University. Series "Biology. Ecology"] 3: 3-11. (in Russian)
- Grachev M.A. 2002. *O sovremennom sostoyanii ekologicheskoy sistemy ozera Baikal*. Novosibirsk: Siberian Branch of the Russian Academy of Sciences. (in Russian)
- Diatomovye vodorosli SSSR. Iskopaemye i sovremennye. Vol. 2, issue 1. 1988. In: Glezer Z.I., Makarova I.V., Moiseeva A.I. et al. (Eds.). *Leningrad: Nauka*. (In Russian)
- Diatomovye vodorosli SSSR. Iskopaemye i sovremennye. Vol. 2, issue 2. 1992. In: Makarova I.V. (Ed.). *SPb: Nauka*. (In Russian)
- Jeong H.J., Park J.Y., Nho J.H. et al. 2005. Feeding by red-tide dinoflagellates on the cyanobacterium *Synechococcus*. *Aquatic Microbial Ecology* 41: 131-143. DOI: 10.3354/ame041131

- Hallegraeff G.M. 2003. Harmful algal blooms: A global overview. In: Hallegraeff G.M., Anderson D.M., Cembella A.D. et al. (Eds.), Manual on harmful marine microalgae. Monographs on oceanographic methodology. Paris, pp. 25-49.
- Harrison W.G. 1976. Nitrate metabolism of the red tide dinoflagellate *Gonyaulax polyedra* Stein. Journal of Experimental Marine Biology and Ecology 21: 199-209. DOI: 10.1016/0022-0981(76)90115-5.
- Jewson D.H., Granin N.G., Zhdanov A.Z. et al. 2009. Effect of snow depth on under-ice irradiance and growth of *Aulacoseira baicalensis* in Lake Baikal. Aquatic Ecology 43: 673-679. DOI: 10.1007/s10452-009-9267-2
- Kamykowski D. 1995. Trajectories of autotrophic marine dinoflagellates. Journal of Phycology 31: 200-208. DOI: 10.1111/j.0022-3646.1995.00200.x.
- Kirchner M., Sahling G., Uhlig G. et al. 1996. Does the red tide-forming dinoflagellate *Noctiluca scintillans* feed on bacteria? Sarsia 81: 45-55. DOI: 10.1080/00364827.1996.10413610.
- Kiselev I.A. 1956. Methods of plankton research. In: Skarlatov O.A. (Ed.), Life in fresh waters of the USSR. Vol 4. Moscow, pp. 140-416. (in Russian)
- Kozhov M.M. 1955. Seasonal and annual changes in Lake Baikal plankton. Trudy Vsesoiuznogo Gidrobiologicheskogo Obshchestva [Proceedings of the All-Russian Hydrobiological Society] 6: 133-157. (in Russian)
- Kozhova O.M. 1957. Horizontal distribution of planktonic algae in Lake Baikal. Izvestia Vostochnykh Filialov Akademii Nauk SSSR [Proceedings of the Eastern Branches of the USSR Academy of Sciences] 4: 5. (in Russian)
- Kozhova O.M. 1959. About the under-ice bloom of Lake Baikal. Botanicheskii Zhurnal [Botanical Journal] 77: 1001-1004. (in Russian)
- Kozhova O.M. 1960. Phytoplankton of Baikal in the area of Listvennichny Bay and its influence on the formation of plankton flora of the Irkutsk reservoir. Izvestia Sibirskogo Otdeleniya Akademii Nauk SSSR [Proceedings of the Siberian Branch of the USSR Academy of Sciences] 12: 120-130. (in Russian)
- Kozhova O.M. 1961. On periodic changes in the development of Lake Baikal phytoplankton. Trudy Vsesoiuznogo Gidrobiologicheskogo Obshchestva [Proceedings of the All-Russian Hydrobiological Society] 9: 28-43. (in Russian)
- Khodzher T.I., Domyshcheva V.M., Sorokovikova L.M. et al. 2017. Current chemical composition of Lake Baikal water. Inland Waters 7: 250-258. DOI: 10.1080/20442041.2017.1329982.
- Kopp C., Pernice M., Domart-Coulon I. et al. 2013. Highly dynamic cellular-level response of symbiotic coral to a sudden increase in environmental nitrogen. mBio 4. DOI: 10.1128/mBio.00052-13.
- Landsberg J.L. 2002. The effects of harmful algal blooms on aquatic organisms. Reviews in Fisheries Science 10: 113-389. DOI: <https://doi.org/10.1080/20026491051695>
- Maguer J.-F., Helguen L., Madec S. et al. 2007. Nitrogen uptake and assimilation kinetics in *Alexandrium minutum* (Dinophyceae): Effect of N-limited growth rate on nitrate and ammonium interactions. Journal of Phycology 43: 295-303. DOI: 10.1111/j.1529-8817.2007.00334x.
- Matvienko O.M., Litvinenko R.M. 1977. Pirofitovi vodorosti — Pyrrophyta. Vyznachnyk presnovodnykh vodorostey Ukrayin'skoyi RSR. Vol. 3, part 2. Kiev: Naukova Dumka. (in Ukrainian)
- Obolkina L.A., Bondarenko N.A., Doroshenko L.F. et al. 2000. On finding a cryophilic community in Lake Baikal. Doklady Akademii Nauk [Proceeding of the Russian Academy of Sciences] 371: 815-817. (in Russian)
- Phillips K.A., Fawley M.W. 2002. Winter phytoplankton blooms under ice associated with elevated oxygen levels. Journal of Phycology 38: 1068-1073. DOI: 10.1046/j.1529-8817.2002.01044.x.
- Popovskaya G.I. Ecological monitoring of phytoplankton in Lake Baikal. 2000. Aquatic Ecosystem Health and Management 3: 215-225. DOI: 10.1080/14634980008657017
- Popovskaya G.I., Genkal S.I., Likhoshvai E.V. 2011. Diatomovye vodorosli planktona ozera Baikal: Atlas-opredelitel'. Novosibirsk: Nauka. (in Russian)
- Roenneberg T., Rehman J. 1996. Nitrate, a nonphotic signal for the circadian system. The FASEB Journal 10: 1443-1447. DOI: 10.1096/fasebj.10.12.8903515
- Rózańska M., Gosselin M., Poulin M. et al. 2009. Influence of environmental factors on the development of bottom ice protist communities during the winter-spring transition. Marine Ecology Progress Series 386: 43-59. DOI: 10.3354/meps08092
- Russell K.M., Galloway J.N., Macko S.A. et al. 1998. Sources of nitrogen in wet deposition to the Chesapeake-Bay region. Atmospheric Environment 32: 2453-2465. DOI: 10.1016/S1352-2310(98)00044-2
- Shimaraev M.N., Verbolov V.I., Granin N.G. et al. 1994. Physical limnology of Lake Baikal: A review. Irkutsk-Okayama: BICER Publishers.
- Smayda T.J. 1997. Harmful algal blooms: Their ecophysiology and general relevance to phytoplankton blooms in the sea. Limnology and Oceanography 42: 1137-1153. DOI: 10.4319/lo.1997.42.5_part_2.1137.
- Spilling K. 2007. Dense sub-ice bloom of dinoflagellates in the Baltic Sea, potentially limited by high pH. Journal of Phytoplankton Research 29: 895-901. DOI: 10.1093/plankt/fbm067.
- Votintsev K.K., Mesheryakova A.I., Popovskaya G.I. 1975. Krugovorot organicheskogo veshchestva v ozere Baikal. Novosibirsk: Nauka. (in Russian)
- Wetzel R.G., Likens G.E. 1991. Limnological analyses. New York: Springer-Verlag.
- Zhai S.J., Yang L.Y., Hu W.P. 2009. Observations of atmospheric nitrogen and phosphorus deposition during the period of algal bloom formation in northern Lake Taihu, China. Environment Management 44: 542-551. DOI: 10.1007/s00267-009-9334-4.
- Zheng T., Cao H., Liu W. et al. 2019. Characteristics of atmospheric deposition during the period of algal bloom formation in urban water bodies. Sustainability 11. DOI: 10.3390/su11061703.